Dynamic Programming based approach for Energy Trading

Avinash Sharma

A Thesis

in

The Department

of

Electrical and Computer Engineering

Presented in Partial Fulfillment of the Requirements

for the Degree of Master of Applied Science (Electrical and Computer Engineering) at

Concordia University

Montreal, Quebec, Canada

February 2018

CONCORDIA UNIVERSITY
SCHOOL OF GRADUATE STUDIES

This is to certify that the thesis prepared

By: Avinash Sharma

Entitled:

Dynamic Programming based approach to Energy Trading

and submitted in partial fulfillment of the requirements for the degree of

Master of Applied Science

Complies with the regulations of this University and meets the accepted standards with respect to originality and quality.

Signed by the final examining committee:

_____ Chair
Dr. R. Raut

_____ Examiner, External
Dr. A. Awasthi (CIISE) To the Program

_____ Examiner
Dr. L.A.C. Lopes

_____ Supervisor
Dr. A.Rathore

Approved by: _____
Dr. W. E. Lynch, Chair
Department of Electrical and Computer Engineering

_____20_____ _____
Dr. Amir Asif, Dean
Faculty of Engineering and Computer Science

Abstract

Dynamic Programming based approach for Energy Trading

Avinash Sharma

Bi-directional Energy Trading is going to play an essential role in facilitating the increased usage of distributed renewable energy sources. The smooth transition towards these clean sources of energy would require opening up of the energy markets to allow for a two-way electricity trade. The study proposes a dynamic programming based energy trading framework (called Dynamic Battery Charging (DBC) Algorithm) from the end-user perspective. Using the proposed energy transfer model the framework finds out the optimal battery charge state at the consumer end. To further improve the performance of the framework, the original DBC algorithm is clubbed together with a capacity fading based battery cost model. For testing and validation purpose, a case study of three different load profiles (different in scale) in three energy markets is done. The simulation results show the profitability of the proposed strategy in all the tested scenarios.

Acknowledgment

I would like to express my sincere gratitude to my supervisor Dr. Akshay K. Rathore for his invaluable support and technical guidance. I am incredibly thankful for his mentorship, patience, support, and willingness to let me pursue research as my interests and the questions led. Thank you, Dr. Rajesh Kumar, for your guidance and encouragement throughout this process. I would like to thank the examination committee: Dr. Anjali Awasthi, Dr. Luiz A. C. Lopes and Dr. Rabin Raut, for their valuable time and insights which helped me towards proper and efficient completion of the work. Finally, thank you to my parents and my brother for your continual love and support.

Publications

- Sharma, A., Kumar, R. and Rathore, A.K. "*A Dynamic Battery Charging Approach for Energy Trading in the Smart Grid.*" In Energy Conversion Congress and Exposition (ECCE), 2018 IEEE. (Accepted)

- Sharma, A., Kumar, R. and Rathore, A.K. "*Dynamic Battery Charging based Energy Trading Framework incorporating Battery Capacity Fading Dynamics.*" In Innovative Smart Grid Technologies-Singapore (ISGT Singapore), 2018 IEEE PES. (Accepted)

Contents

List of Figures

List of Tables

List of Algorithms

List of Symbols

t	Time Slot
p_t	Electricity Price (in \$/Wh) at t
b_t	Battery Charge (in Wh) at t
Δb_t	Change in b (in Wh) at t
d_t	Load demand (in Wh) at t
s_t	Generated Renewable energy (in Wh) at t
u_t	Energy traded (in Wh) from utility at t
$b^{capacity}$	Battery Capacity (in Wh)
b^{min}	Reserved Battery Charge (in Wh)
db^{crate}	Maximum Battery Charging Rate (in W)
db^{drate}	Maximum Battery Discharging Rate (in W)
β_1	Price Coefficient
β_2	Energy Loss Coefficient
β	Trading coefficient
ℓ_t	Monetary Loss (in \$) at t
ℓ_{total}	Total Monetary Loss (in \$) at t
ℓ_{av}	Average Monetary Loss (in \$) at t
T	Number of Time Slots used for each estimation
τ	Current Time Slot
$E_p[p_t;\tau]$	Estimation of p_t at time slot τ
$E_d[d_t;\tau]$	Estimation of d_t at time slot τ
$E_s[s_t;\tau]$	Estimation of s_t at time slot τ

L	Loss Function
t_f	Total Number of Time Slots
f_τ	Minimization Problem at τ
$b^*(\tau)$	Optimal Battery Charge
F_τ	Objective Function at τ
c_1	Reserve Battery Penalty Coefficient
c_2	Battery Capacity Penalty Coefficient
c_3	Battery Charging Rate Penalty Coefficient
c_4	Battery Discharging Rate Penalty Coefficient
c_5	Battery Discharge Penalty Coefficient
L_y	Yearly Monetary Loss (in $\$/year$)
p_1	Yearly Monetary Profit using PV and Battery(in $\$/year$)
p_2	Yearly Monetary Profit using Battery(in $\$/year$)
c	Number of Cycles
GP	Gross Profit in $in\$$
$\%GP$	Percentage Gross Profit $in\%$
f_d	Capacity Fading Rate
S_{av}	SOC Mean
S_{dv}	SOC Standard Deviation
Ah	Battery Charge
ΔAh	Change in Battery Charge
$k_1 - k_4$	Battery Capacity Fading Model Parameters
$\%f_d$	Percentage of Battery Capacity fade per year
c_{f_d}	Battery Cost Function (in \$)
B_{cost}	Battery System Cost
cpf	Cost per Fade Factor (in $\$/Wh$)
w_f	Fading Cost Coefficient

Chapter 1

Introduction to Energy Trading

1.1 Introduction

Last decade has witnessed a lot of changes in the energy sector around the world. With the rapid rise in human population, an increasingly energy dependent human lifestyle, industrial automation and a shift towards Electric Vehicles (EVs), the energy demand has seen a drastic growth all around the world. Even by the conservative estimation, by 2050 the world population would rise by **23**% to 8600 million (Figure 1.1) with a GDP per capita rise of at least **40**% (Figure 1.2). If the above World Energy Council (WEC) estimates[1] are to be believed, by the year 2050, the energy consumption would increase by at least **30**% (Figure 1.3). The WEC estimations are for two future world scenario. The **'Symphony'** scenario assumes that the future energy infrastructure would continue to be operated in a centralized manner by the government and the **'Jazz'** scenario assumes a wide scale decentralization of the energy infrastructure.

This would require a substantial increase in the electricity generation from both conventional and non-conventional energy sources. But the conventional fossil fuel based sources are not without problems. Man-made problems like global warming and increased greenhouse emission are generally associated with these conventional energy sources. Further, the recent studies[2–4] have shown the long-term benefits of the renewable energy sources on economic growth of a country. All this together has resulted in growing unpopularity of these conventional sources.

The recent advancements in the grids promise unprecedented improvements in the energy efficiency. But even if the energy efficiency aspect is considered, it would not be

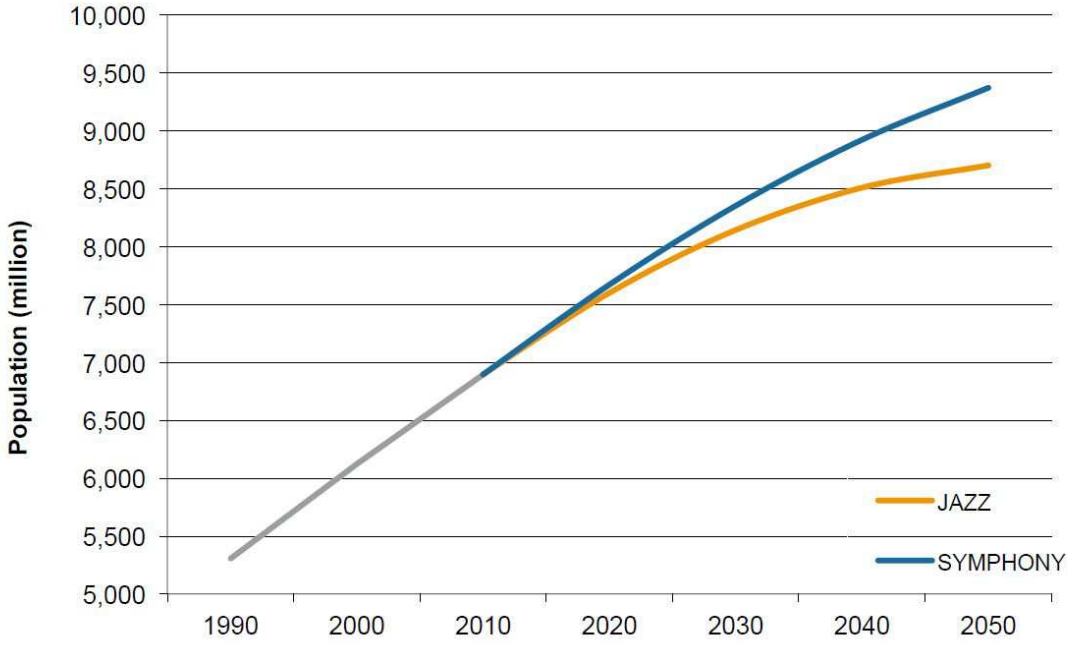

Figure 1.1: WEC - Estimated Population Growth [1]

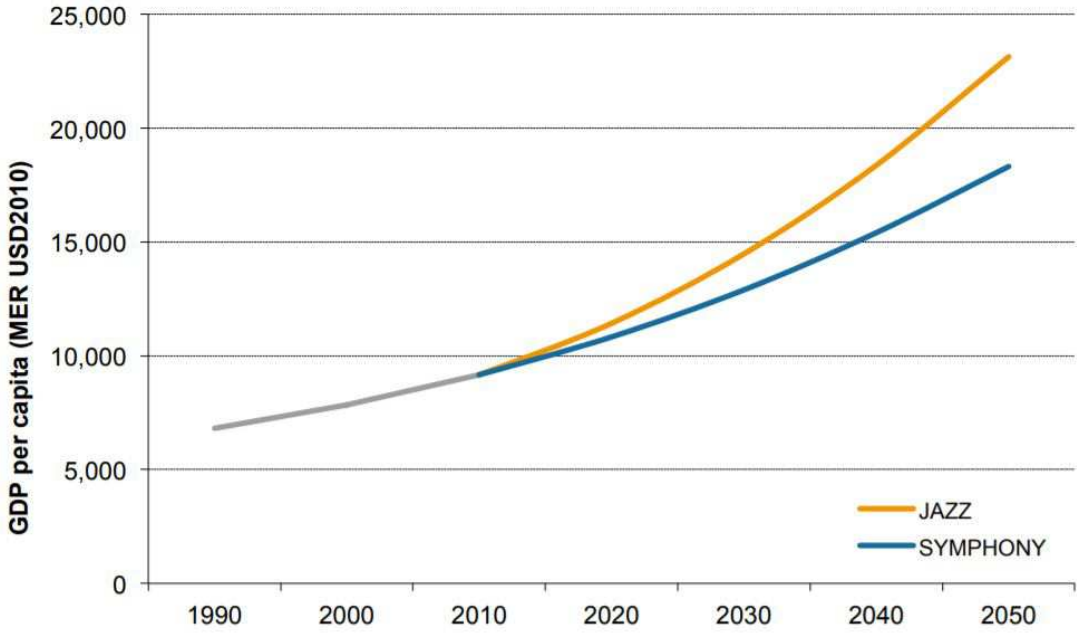

Figure 1.2: WEC - Estimated GDP per Capita Growth [1]

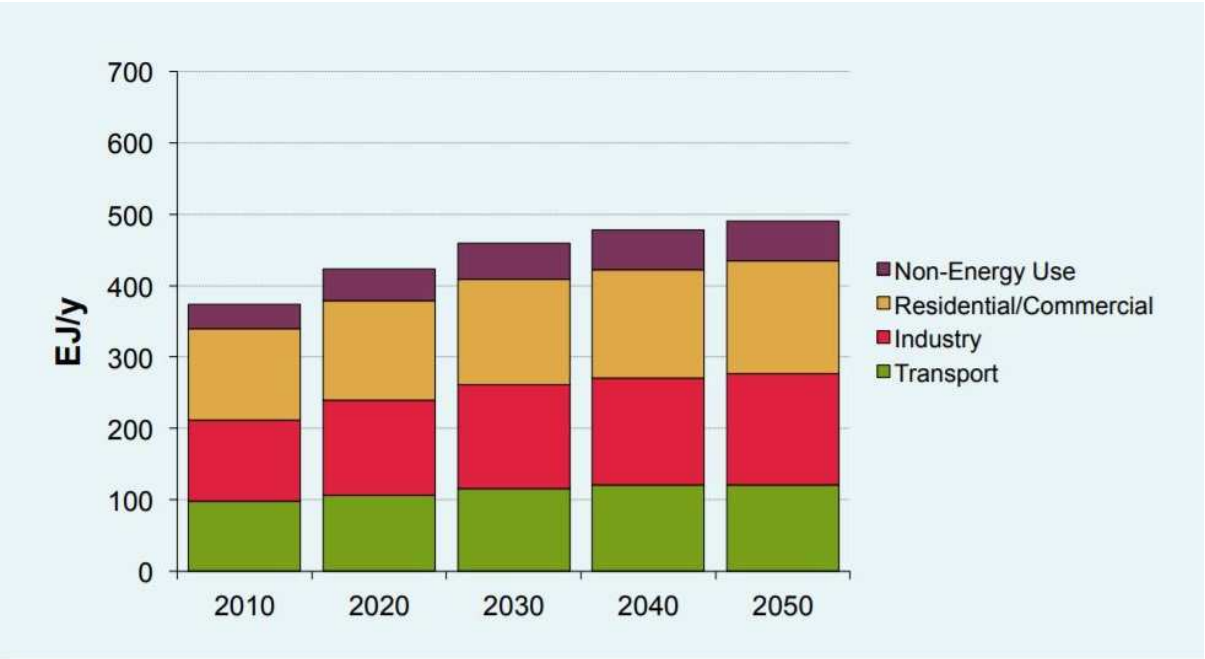

Figure 1.3: WEC - Total Energy Consumption by Sector [1]

enough to fulfill the future energy demand. The deployment of decentralized generation and storage technologies are going to play a significant role in satisfying the future demand. The front-runner in this shift towards decentralization is the solar power, which would allow for a large-scale decentralization of the energy generation and distribution process. The pressure and challenge to further improve and transform the energy infrastructure is immense. Further, the future policymakers and business leaders would require taking critical decisions to tackle the future uncertainties in the energy infrastructure.

This change towards decentralized renewable sources, although inevitable, requires a large scale and efficient integration with the present electricity systems[5, 6]. However, this process is not without problems. Renewable sources like solar and wind power tend to be highly unpredictable and unstable. They tend to vary in electricity generation with no correlation to the changes in electricity demand. Further, the conventional power grids are not flexible enough, and due to their highly centralized and homogeneous nature, increased integration of renewable energy can lead to stability and reliability issues in the system[7–10]. The future penetration of renewable sources is rather unavoidable. This calls for a shift towards more sophisticated smart grid based electricity grid networks[11–14]. In general, a smart grid is a network that allows the small-scale producers to generate and sell electricity. In contrast to the conventional grid networks, these networks are het-

erogeneous and decentralized in nature and incorporate a variety of resources like smart meters, intelligent power distribution devices, two-way communications, advanced sensors, and energy storage systems. These resources together would facilitate the increased penetration of renewable sources, electric vehicles, and micro-grids into the present electricity infrastructure. This would require the current infrastructure to develop an ability for the end-user to participate in the decentralized bilateral energy trade to partially fulfill their needs without further stressing the grid.

However, this shift towards smart grid requires increased participation by the consumers in the process of electricity generation and distribution. To facilitate this transition, the energy markets would have to be a lot more open, decentralized and must allow the end-users to sell the surplus electricity back to the grid as well as to the other end-users. Demand side management and response mechanisms would be an integral part of this system[15, 16]. In this respect, energy storage units like battery are going to play a significant role in incentivizing the consumer for adopting locally available renewable sources like solar power[17, 18]. These units allow the participating user to store energy as a reserve or for enabling smart energy trade. However, deployment of storage units in the system comes with its problem, both for the overall grid system and for the consumer[19–21]. The issues can range from economic viability to system stability. However, the rapidly decreasing cost of battery systems[22, 23] in the recent years has made them a lot more attractive and economically feasible to be deployed for use in small-scale PV systems. Companies like Tesla are investing heavily in improving the battery technology and further reducing their overall cost. As in [22], the battery price has declined at a rate of $\mathbf{14}\%$ annually and has already reached below $\mathbf{300\$/kWh}$ price level. Recent events like negative electricity pricing in California due to massive solar energy influx, further confirms the prospect of energy trading to be attractive.

1.2 Why Energy Trading?

1.2.1 Better Overall Efficiency

The penetration of renewable energy comes with its baggage of problems due to its inherent uncertainty. But due to its highly decentralized nature and associated use of storage systems along with it, the energy trading could allow the system operator to

provide various ancillary services to improve the overall efficiency of the system. Further, due to localized generation, the transmission line congestion would reduce resulting in an overall improvement of the efficiency and reduction in average cost.

1.2.2 Reduced Operation Cost

The operating cost of the utilities is generally decided by the overall load demand. In general, they operate large-scale, low-cost generating units for the base demand and dispatch more generators to keep up with the changing end-user demand. During peak hours the utilities have to deploy high cost and faster gas power stations, which results in increased operating cost with an increase in the load demand. So, to deal with the higher operating cost, utilities have to increase the electricity price. If the energy trading is allowed, both the utility and the users will benefit in the form of cost savings [24].

1.2.3 Reduced Green House Gas (GHG) Emissions

Power grids around the world are responsible for **25**% of the GHG emissions. The increased usage of decentralized energy can play a critical role in reducing the GHG emissions. This can mainly be realized by enabling the energy trade for the excess power at the micro-grid level.

1.2.4 Energy Profiling

The energy trading inherently allows for generation decentralization. This would lead to the emergence of networked micro-grids. These micro-grids would enable the central grid to better profile the end-user demand and control the flow and generation of energy. This would allow for a better system adaptation towards future energy demand and CO_2 targets. Instead of relying on centralized utility companies to build capital-intensive, large-scale power plants, the micro-generation network can enlarge the electricity supply at a cost-effective, small-scale local level.

1.3 Objective

The increasing energy demand and various problems surrounding the conventional energy sources, has made the shift towards distributed renewable energy sources inevitable. But the high infrastructural costs can be demotivating for the end-users to make this shift. The objective of this work is to come up with an energy trading framework to enable the end-user to generate profits by trading electricity with a smart grid where the energy network has evolved enough to facilitate bi-directional energy trading.

1.4 Problem Statement

The smart grid with its inherent bi-directional electricity trading capability facilitates the end-user to decide the amount of energy to trade. By trading electricity smartly, the end-user can easily offset the battery system investment cost. But this requires the development of an energy trading framework that by forecasting electricity price, load demand and solar harvest, can decide the optimal amount of electricity to buy or sell over a period of time so as to generate a net profit while recovering the battery investment cost quickly.

1.5 Thesis Layout

In this work, a detailed study about the use of battery systems for energy trading was conducted from the end-user perspective by incorporating battery dynamics in the form of constraints in the overall energy trading framework. This was formulated in terms of an energy trading model. Further, a strategy called Dynamic Battery Charging Algorithm (DBC) was developed to find the optimal battery charging states during the overall trading process. For validating the performance of the proposed strategy, the algorithm was tested on nine different cases. For this, a case study of three different load profiles (a small scale residential user, a Walmart Supercenter as a medium scale commercial user and an automotive assembly unit as a large-scale industrial user) was done. Further, all three profiles were tested in three electricity spot markets in different states (Ontario, California and New York). Using the real-time traces, three estimators were trained for predicting one hour-ahead price, solar power, and load demand. This was used to test

and validate the proposed strategy in real time scenarios.

In Chapter 2 discusses the various energy trading methods existing in the literature. Chapter 3 formulates the core DBC based energy trading approach. Further, it shows the simulation results of the proposed strategy in the 9 test cases. Chapter 4 formulates a capacity fade based battery cost model and utilizes it within the core DBC algorithm to model the battery utility cost model within it. In chapter 5 the proposed DBC and capacity fade based hybrid model is further improved by using weighted capacity fade battery cost model. Finally, chapter 6 concludes the overall study.

Chapter 2

Literature Survey

2.1 Energy Trading Survey

To incentivize the battery usage among end-user, we need to come up with proper trading strategies to enable the user to participate and gain profit in an open energy market. Researchers are working on different such strategies in various market conditions. In general, the energy trading can be classified into three main categories depending on the employed solution strategy as described below:

2.1.1 Decentralized Approach:

This is a Game Theoretic Approach which assumes multiple interacting users who try to optimize their own utilities without considering the rest of the user and the grid conditions. This approach can be further divided into three subcategories:

- **Auction Mechanism:**

  The primary goal of this strategy is to find the lowest cost matching between supply and demand to maximize the economic efficiency. In [25], a basic auction mechanism for trading in the local energy markets is proposed. In [26] authors proposed a double auction based energy trading mechanism. In [27], a Continuous Double Auction (CDA) based mechanism is used for congestion management with a micro-grid based energy trading scenario. In [28], the authors modeled the energy trading process between the distributed storage units using a double auction based strategy. [29] authors formulated the energy exchange between Electric vehicles and grid. The

model utilizes a double auction based energy trading strategy.

- **Stackelberg Game:**

  A stackelberg game models the trading process as a leader-follower based response strategy. The game models the behavior of leader and follower. The leader is given the first move advantage, and follower plays the best possible response based trading strategy so as to maximize its utility [30]. In energy trading field the role of a leader is played by the utility which sets the electricity prices as per the market requirements and the follower role is played by the end-users. In [31], the utility motivates the end-users to sell their surplus energy during the peak hours. In [32], the authors modeled the energy exchange between vehicle and grid using the leader-follower based Stackelberg Game.

- **Non-cooperative Game:**

  A non-cooperative game models the energy trading process as the interaction between independent self-interested agents. In this strategy, the non-cooperative games are used to estimate the net energy to be sold in the market. The optimal solution is the Nash Equilibrium, where no player deviates from its strategy. This approach has been used in a lot of work [33–36] to solve derive an optimal energy exchange strategy in various scenarios. In [36], a non-cooperative game between storage units is proposed and is solved using a game theory-based approach. In [34], a non-cooperative game is utilized to find the optimal energy exchange between plug-in hybrid vehicles.

2.1.2 Centralized Approach:

In this approach the utility or trading agency is assumed to know all the information about the buyers and sellers. The approach utilizes a single objective maximization based strategy to estimate the optimal amount of energy to be traded. In [37] a profit maximization strategy is proposed for micro-generation unit working in a mostly centralized market with incentives for energy trading. In [38], authors analyzed an energy trading scenario in a peer-to-peer network for energy exchange between micro-grids where a central grid has all the information about individual micro-grid. In [39], authors proposed a heuristic approach called Hybrid Immune Algorithm, for auction based distributed energy resource

management in Smart Grid. In [40], authors formulated a stochastic programming based approach to select optimal energy and reserve bids for the storage units while working in a scenario where a group of independently-operated investor-owned storage units seeks to offer both energy and reserve.

2.1.3 Simulation-based Approach:

This approach models and simulates the behavior of multiple agents. These strategies utilize various statistical algorithms like Reinforcement learning so as to automate [41, 42] the decision making process with a motive of maximizing the profit. In [43], B–M reinforcement scheme[44] is used to attain Nash equilibrium in a constrained energy trading game between players with incomplete information. Various other approaches [45, 46] have utilized Reinforcement learning based strategies for this purpose. In [47], the authors utilized Markov decision process to model the broker agent behavior.

Chapter 3

Dynamic Battery Charging based Energy Trading

In this chapter, an energy trading framework called **Dynamic Battery Charging (DBC)** Algorithm is proposed. The chapter includes a detailed study regarding the use of the battery systems for energy trading from the end-user perspective. The proposal incorporate the battery dynamics in the form of constraints in the overall energy trading framework. The framework utilizes an energy balance based trading model called **Energy Transfer Model** within it. Finally, the **DBC** Algorithm is developed to find the optimal battery charging states during the overall trading process. For validating the performance of the proposed framework, the algorithm is tested on nine different scenarios. For this, a case study of three different load profiles (a small scale **Residential** user, a Walmart Supercenter as a medium scale **Commercial** user and an automotive assembly unit as a large-scale **Industrial** user) is done. Further, all three profiles are tested in three electricity spot markets in different states (**Ontario**, **California** and **New-York**). Using the real-time traces, three estimators are trained for predicting one hour-ahead price, solar power, and load demand. This was used to test and validate the proposed framework in the real-time scenarios.

3.1 Energy Transfer Model Formulation

The proposed model considers the trading operation from the end-user perspective. The end-user is directly connected to a central smart grid system that allows a two-way

electricity trade. The model formulates the monetary loss incurred by the end-user while buying or selling the electrical power over a particular time-period. All the variables are considered to be discrete with each time-slot taken as $\mathbf{1}$ hour and denoted by '$\boldsymbol{t}$'. For example, $\boldsymbol{p_t}$ indicates the average one-hour spot market price of the electricity in the time slot $\boldsymbol{t}$. The spot market prices are taken from **IESO**[48], **CAISO**[49], and **NYISO**[50] for the Ontario, California and New-York states respectively. Figure 3.1 represents the overall system energy transfer model. The system consists of a load, a PV system for electricity generation, a battery to store energy and a central utility to buy energy deficit or sell energy surplus. Here $\boldsymbol{d_t}$ denotes the load energy requirement in the time slot $\boldsymbol{t}$. $\boldsymbol{s_t}$ denotes the solar energy harvested using the PV system (excluding the energy loss during the harvesting process) in time slot $\boldsymbol{t}$.

$\boldsymbol{b_t}$ indicates the initial charge of the battery (at the start of time slot $\boldsymbol{t}$), and $\boldsymbol{\Delta b_t}$ denotes the change in charge of the battery in time slot $\boldsymbol{t}$. Positive $\boldsymbol{\Delta b_t}$ denotes charging of the battery while negative $\boldsymbol{\Delta b_t}$ denotes discharging of the battery. This change can be formulated as Eq.(3.1).

$$b_{t+1} = b_t + \Delta b_t \tag{3.1}$$

$\boldsymbol{b^{capacity}}$ represents the maximum charge accumulation capacity of the battery and $\boldsymbol{b^{min}}$ represents the reserved battery charge. Thus in any time-slot $\boldsymbol{t}$ the battery charge cannot go beyond this range. Eq.(3.16) accounts for this constraint.

As represented by the Eq.(3.17), $\boldsymbol{\Delta b_t}$ is limited by maximum charging rate ($\boldsymbol{db^{crate}}$) and maximum discharging rate ($\boldsymbol{db^{drate}}$).

Eq.(3.18), limits the battery discharge ($-\boldsymbol{\Delta b_t}$) in slot $\boldsymbol{t}$ to remain within the present battery charge.

$\boldsymbol{u_t}$ denotes the amount of electricity traded from the utility in time slot $\boldsymbol{t}$. Positive $\boldsymbol{u_t}$ indicates that energy is brought from the utility while its negative value denotes that the energy is sold to the utility.

The total energy supply and energy demand in a system (Figure 3.1) are always balanced. This can be formulated as Eq.(3.2).

$$u_t + s_t = \Delta b_t + d_t \tag{3.2}$$

The variable $\boldsymbol{p_t}$ denotes the price at which the end-user can buy the electricity from the grid. Whenever the energy is bought from the grid ($\boldsymbol{u_t} \geq \mathbf{0}$), the end-user incurs a

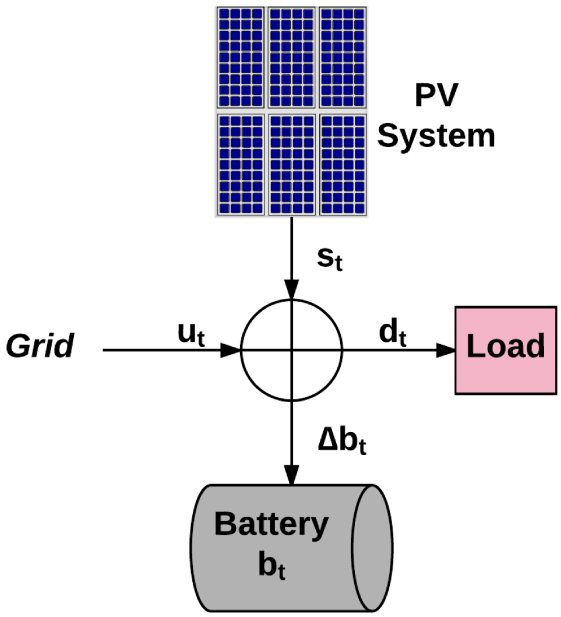

Figure 3.1: System Energy Transfer Model

net monetary loss represented by $p_t * u_t$. Compared to that, the selling price is assumed to be less than p_t. This is to factor in the cost incurred by the central grid for running the energy market. This can be formulated by using a constant parameter called price coefficient (β_1) with a value between 0 and 1. So, in this case, the selling price is taken as $\beta_1 * p_t$. Further, there exists an energy loss (AC/DC conversion loss and transmission loss) when selling the electricity to the grid. This loss is approximated by using another constant parameter called energy loss coefficient (β_2). So, the net energy sold in this case can be approximated as $\beta_2 * u_t$. While selling ($u_t \leq 0$), the end-user gains a profit which can be represented in terms of negative loss as $\beta_1 * \beta_2 * p_t * u_t$. Overall, the monetary loss (ℓ_t) incurred in time slot t is formulated as given by Eq.(3.3).

$$\ell_t = \begin{cases} p_t * u_t & \text{if } u_t \geq 0 \\ \beta_1 * \beta_2 * p_t * u_t & \text{if } u_t < 0 \end{cases} \tag{3.3}$$

The two trading situations are combined by taking another parameter called trading coefficient (β) as represented in Eq.(3.4).

$$\beta = \begin{cases} 1 & \text{if } u_t \geq 0 \\ \beta_1 * \beta_2 & \text{if } u_t < 0 \end{cases} \tag{3.4}$$

This can be used to combine the two conditions in Eq.(3.3) to form monetary loss equation as shown in Eq.(3.5).

$$\ell_t = \beta * p_t * u_t = \beta * p_t * [\Delta b_t + d_t - s_t] \tag{3.5}$$

The Eq.(3.6) represents the total monetary loss ℓ_{total} incurred by the end-user.

$$\ell_{total} = \sum_t \beta * p_t * [\Delta b_t + d_t - s_t] \tag{3.6}$$

The objective of every end-user based strategy is to minimize this monetary loss or rather gain a significant profit. This can also be achieved by minimizing the average monetary loss ℓ_{av} as represented by Eq.(3.7).

$$\ell_{av} = \lim_{T \to \infty} \frac{1}{T} \sum_t \beta * p_t * [\Delta b_t + d_t - s_t] \tag{3.7}$$

The Eq.(3.8) represents the average monetary loss incurred by the end-user during $\boldsymbol{T}$ consecutive time slots starting from time slot ($\boldsymbol{\tau}$).

$$\ell_{av}(\tau, T) = \frac{1}{T} \sum_{t=\tau}^{\tau+T-1} \beta * p_t * [\Delta b_t + d_t - s_t] \tag{3.8}$$

For calculating $\ell_{av}(\boldsymbol{\tau}, \boldsymbol{T})$ (as given in Eq.(3.8)), the accurate values of $\boldsymbol{p_t}$, $\boldsymbol{\Delta b_t}$, $\boldsymbol{d_t}$ and $\boldsymbol{s_t}$ are required to be known for time slots $\boldsymbol{\tau}$, $\boldsymbol{\tau + 1}$.... and $\boldsymbol{\tau + T - 1}$ at time slot τ. This can be approximated by estimating the price ($\boldsymbol{p}$), load demand ($\boldsymbol{d}$) and harvested solar energy ($\boldsymbol{s}$) for all the future time slots. $\boldsymbol{p_t}(\boldsymbol{\tau})$, $\boldsymbol{d_t}(\boldsymbol{\tau})$ and $\boldsymbol{s_t}(\boldsymbol{\tau})$ in Eq.(3.9), (3.10) and (3.11) represent the forecasted estimations of $\boldsymbol{p_t}$, $\boldsymbol{d_t}$ and $\boldsymbol{s_t}$ at $\boldsymbol{\tau}$ time slot.

$$p_t(\tau) = E_p[p_t; \tau] \tag{3.9}$$

$$d_t(\tau) = E_d[d_t; \tau] \tag{3.10}$$

$$s_t(\tau) = E_s[s_t; \tau] \tag{3.11}$$

By using above estimations, the Eq.(3.8) can be approximated as a function of the change in battery charge. This leads to the loss function given in Eq.(3.12).

$$\begin{aligned} L(\Delta b(\tau); \tau, T) &\approx \ell_{av}(\tau, T) \\ &\approx \frac{1}{T} \sum_{t=\tau}^{\tau+T-1} \beta * p_t(\tau) * [\Delta b_t(\tau) + d_t(\tau) - s_t(\tau)] \end{aligned} \tag{3.12}$$

Here, $\boldsymbol{\Delta b}(\boldsymbol{\tau}) = [\boldsymbol{\Delta b_\tau}(\boldsymbol{\tau}), \boldsymbol{\Delta b_{\tau+1}}(\boldsymbol{\tau}), ..., \boldsymbol{\Delta b_{\tau+T-1}}(\boldsymbol{\tau})]$. By minimizing the loss function (Eq.(3.12)) for different time slot pairs ($\boldsymbol{\tau}$, $\boldsymbol{T}$), we can achieve the end-user task of reducing the overall monetary loss. This would give the optimal values of battery charge for different time slots.

3.2 Dynamic Battery Charging Algorithm (DBC)

Let t_f be the total number of time slots for which we have to predict the battery charge state. The aim of the DBC algorithm is to accurately estimate these values. Prior to estimating the optimal battery charge values, three separate time series estimators, E_p, E_d and E_s, are trained for price, load and solar power prediction. For this a machine learning technique called Support Vector Machine [51] was used to train the three time series regression models [52–54]. At any time slot τ, these time series estimators can be used to predict the values of p_t, d_t and s_t for future time slots ($t > \tau$).

$$f_\tau : \min_{\Delta b(\tau)} \frac{1}{T} \sum_{t=\tau}^{\tau+T-1} \beta * p_t(\tau) * [\Delta b_t(\tau) + d_t(\tau) - s_t(\tau)] \quad s.t.((3.16)), ((3.17)), ((3.18)) \tag{3.13}$$

$$\Delta b^*(\tau) = \operatorname*{argmin}_{\Delta b(\tau)} \frac{1}{T} \sum_{t=\tau}^{\tau+T-1} \beta * p_t(\tau) * [\Delta b_t(\tau) + d_t(\tau) - s_t(\tau)] \quad s.t.((3.16)), ((3.17)), ((3.18)) \tag{3.14}$$

$$b^*_\tau = b^*_{\tau-1} + \Delta b^*_\tau(\tau) \tag{3.15}$$

$$b^{min} \leq b_t \leq b^{capacity} \tag{3.16}$$

$$db^{drate} \leq \Delta b_t \leq db^{crate} \tag{3.17}$$

$$-\Delta b_t \leq b_t - b^{min} \tag{3.18}$$

$$\begin{aligned} F_\tau(\Delta b) = \frac{1}{T} \sum_{t=\tau}^{\tau+T-1} & [\beta * p_t(\tau) * [\Delta b_t(\tau) + d_t(\tau) - s_t(\tau)] \\ & + c_1 * (b(t) - b^{min})^2 + c_2 * (b^{capacity} - b(t))^2 \\ & + c_3 * (\Delta b(t) - db^{drate})^2 + c_4 * (db^{crate} - \Delta b(t))^2 \\ & + c_5 * (b(t) + \Delta b(t) - b_{min})^2] \end{aligned} \tag{3.19}$$

The Eq.(3.13) represent the minimization problem at a particular time-slot "τ". So, in total there are t_f different minimization problems from time slots $\tau = 1$ to $\tau = t_f$.

Algorithm 1 DBC

1: Train Estimators: E_p, E_d and E_d.
2: **for** $\tau = 0 : t_f$ **do**
3: **for** $t = \tau + 1 : \tau + T$ **do**
4: Estimate $p_t(\tau)$, $d_t(\tau)$ and $s_t(\tau)$
5: Solve f_τ using optimizer
6: $b^*_\tau \leftarrow b^*_{\tau-1} + \Delta b^*_\tau(\tau)$

Solving the minimization problem ($\boldsymbol{f_\tau}$) at particular time slot $\boldsymbol{\tau}$ yields the optimal battery charge update (Eq.(3.14)) from $\boldsymbol{t = \tau}$ to $\boldsymbol{t = \tau + T - 1}$ w.r.t. to the present time slot $\boldsymbol{\tau}$. In Eq.(3.14), $\boldsymbol{\Delta b^*(\tau) = [\Delta b^*_\tau(\tau), \Delta b^*_{\tau+1}(\tau), ..., \Delta b^*_{\tau+T-1}(\tau)]}$. Of these, the battery charge values for future time slots ($\boldsymbol{t > \tau}$) are affected by inaccuracies in predictions of price, load and solar power. So, these later values are discarded and the change in battery charge at $\boldsymbol{\tau}$ ($\boldsymbol{\Delta b^*_\tau(\tau)}$) is used to calculate the optimal battery charge at that time slot (Eq.(3.15)). By solving the minimization problem for all time slots, the required optimal battery charge pattern can be obtained. Eq.(3.19) represents the overall minimization objective function ($\boldsymbol{F_\tau}$) incorporating all the battery constraints (Eq.(3.16),(3.17),(3.18)). This is done by adding a penalty to the objective function whenever any of the constraint is violated. $\boldsymbol{c_1}$, $\boldsymbol{c_2}$, $\boldsymbol{c_3}$, $\boldsymbol{c_4}$ and $\boldsymbol{c_5}$ are penalty coefficients for these constraints. They are given a positive value if the respective constraint is violated else they are $\boldsymbol{0}$. The overall algorithm is presented in Figure 3.2.

Any iterative optimization algorithm can be used to solve $\boldsymbol{f_\tau}$ in step 5 of the Algorithm 1. All the iterative optimization algorithms can be classified into two main types: gradient based and non-gradient based. Both of these optimization algorithms are tested in this work. In this work, both types of optimization algorithms are tested with momentum-based gradient descent (MGD) representing the gradient-based method [55] and differential evolution (DE) [56] representing non-gradient method. Compared to other optimization algorithms, these algorithms are computationally faster and easier to implement. Further, they are known to work well in multimodal optimization problems.

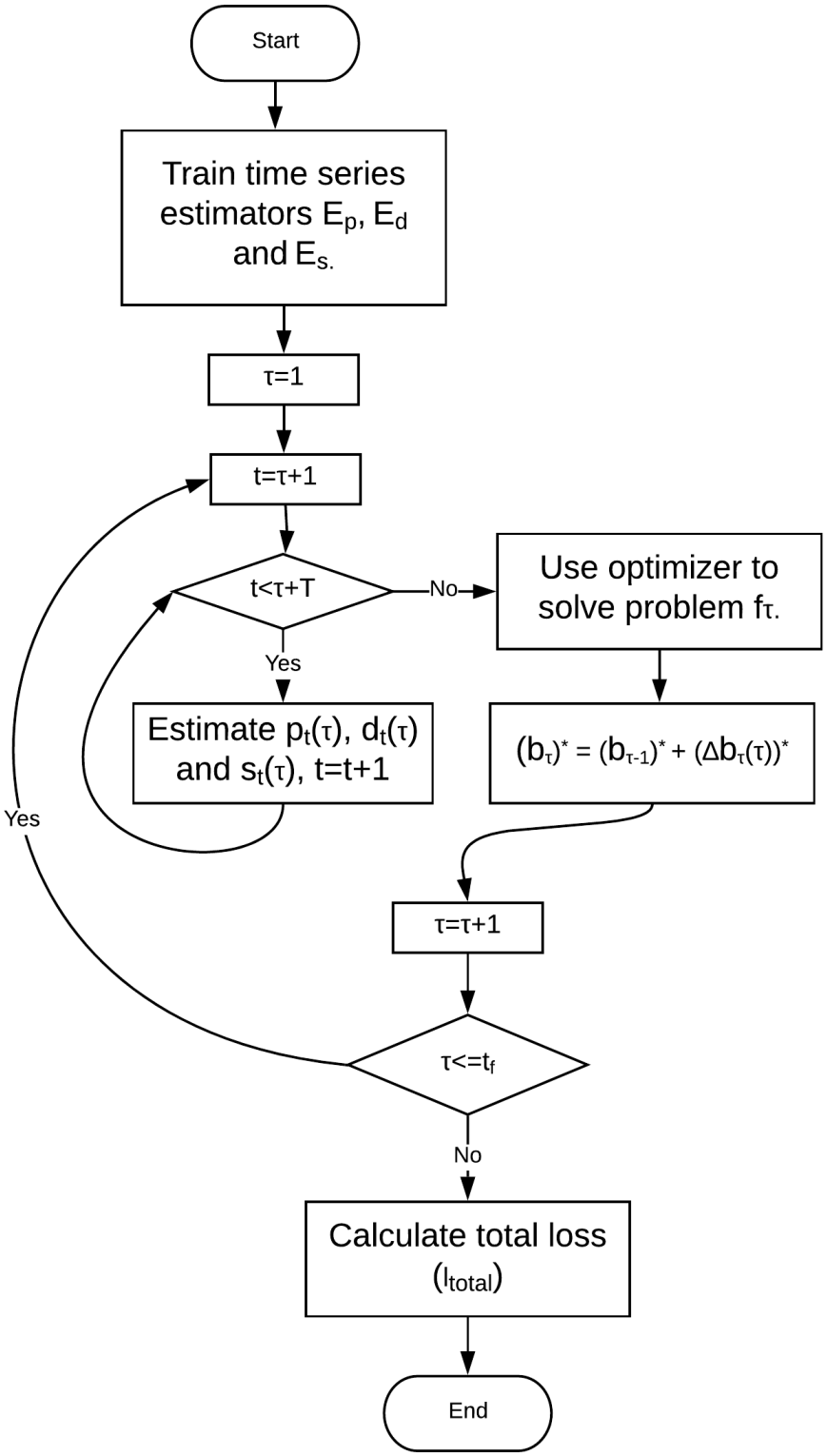

Figure 3.2: DBC Algorithm Flowchart

3.3 Solution Strategies Overview

In the study, three different end-user strategies are tested based on the electricity generation and storage hardware possessed by the end-user. These strategies are classified as "Without Solar Harvesting Strategy", "Greedy Strategy" and "Smart Strategy".

3.3.1 Without Solar Harvesting Strategy

This represents the case where the end-user does not possess a solar harvesting system and just buys all the required electricity directly from the grid. The monetary loss value for this situation is calculated as Eq.(3.20).

$$\ell_{total} = \sum_{t} p_t * [d_t]. \tag{3.20}$$

3.3.2 Greedy Strategy

This represents the case where end-user does have a solar system but don't use a battery for energy trading. In this situation, the end-user just sells the extra solar energy to the grid or buys the demand deficit from it. The monetary loss value for this situation is calculated as Eq.(3.21).

$$\ell_{total} = \sum_{t} p_t * [d_t - s_t] \tag{3.21}$$

3.3.3 Smart Strategy

In this case, the end-user possess both a solar system and a battery and uses an algorithm to smartly use the battery for energy trading. This strategy is tested with three different algorithms: Reinforcement Learning, DBC algorithm with DE and DBC algorithm with MGD. These algorithms can be used as follows:

- **Reinforcement Learning:**

  Reinforcement learning (RL)[57] is a trail-and-error based technique that continuously trains an agent using its behavioral samples in a particular environment and using that it drives the agent behavior towards optimality w.r.t. that environment. These samples are taken by enabling the agent to take actions ($\boldsymbol{u_t}$) in the form of interactions with its environment. These interactions result in a change of state

($\boldsymbol{b_t}$) of the agent. By taking these actions the agent gets a reward ($\boldsymbol{r_t}$ as given in Eq.(3.22)) which can then be used to calculate cumulative reward ($\boldsymbol{R}$) using Eq.(3.23). The algorithm makes use of these accumulated reward values to train the agent to return better rewards in future. In our case, the monetary profits can be used as reward function, and the battery charge can be used as the agent state. Change in battery state is used as the action which is represented by using a policy function ($\boldsymbol{\pi}$). One class of the RL algorithm is an iterative approach called Q-learning. Q-learning starts with randomly generating Q-value of the policy or a reference value of the policy set by the designer. Every time the agent selects an action, it observes a reward and a new state that may depend on both the previous state and the chosen action and updates the corresponding Q-value using the Eq.(3.24).

$$r_{t+1} = r(b_{t+1}|b_t, u_t) \tag{3.22}$$

$$R(T) = r_T(b_T) + \sum_{t=1}^{T-1} r_t(b_t, u_t) \tag{3.23}$$

$$\begin{aligned} Q_{t+1}(u_t, b_t) \quad &= Q_t(u_t, b_t) + \alpha_t(u_t, b_t)(r_{t+1} + \\ &\gamma \max_a Q_t(b_{t+1}, u) - Q_t(b_t, u_t)) \end{aligned} \tag{3.24}$$

Here $\boldsymbol{\gamma}$ is discount factor between $\mathbf{0}$ and $\mathbf{1}$. The most popular way to implement Q-leaning is to use neural networks as a function approximator to approximate the policy function ($\boldsymbol{\pi}$). This method implemented in [58] is called Deep Q-learning with Experience Replay. The overall algorithm can be implemented as given in Algorithm 2.

- **DBC algorithm with Differential Evolution (DE):**

  Differential Evolution (DE)[56] is a non-gradient based iterative optimization technique that belongs to the class of algorithms called evolutionary computation. These algorithms are based on the theory of evolution. DE tries to solve a problem by iteratively improving a set of candidate solutions. The candidate population moves in the search space iteratively by three evolutionary steps (Mutation, Crossover and

Algorithm 2 Deep Q-learning with Experience Replay

Initialize the experience-replay buffer (B) of size N_B.
Initialize high ϵ value (ϵ greedy approach).
Initialize the deep neural network representing policy or state-action Q value.
for $k = 1 : N_e$ **do**
    Initialize system state as b_1.
    while Until Episode is Completed **do**
        Generate random number rn between 0 and 1.
        if $rn \leq \epsilon$ **then**
            Generate random action u_t
        else
            $b_t \leftarrow \max_u Q^*(b_t, u)$
        Use action u_t to get reward r_t and new state b_{t+1}.
        Update B using sample (b_t,u_t,r_t,b_{t+1}).
        Create minibatch(mb) of random samples from B.
        for Each sample x_i=(b_i,u_i,r_i,b_{i+1}) in mb **do**
            if o_{i+1} ends k^{th} episode **then**
                $y_i \leftarrow r_i$
            else
                $y_i \leftarrow r_i + \max_{u'} Q^*(b_{t+1}, u')$
        Update the deep neural network parameters using minibatch samples.
    Decrease ϵ value.

Selection) given in Eq.(3.25), Eq.(3.26) and Eq.(3.27).

$$v_i = x_a + F.(x_b - x_c) \tag{3.25}$$

$$u_i = \begin{cases} v_i & \text{if } r_j \leq CR \text{ or } j = I_r \\ x_i & \text{if } r_j > CR \text{ or } j \neq I_r \end{cases} \tag{3.26}$$

$$x_i = \begin{cases} u_i & \text{if } F_\tau(u_i) \leq F_\tau(x_i) \\ x_i & \text{if } F_\tau(u_i) > F_\tau(x_i) \end{cases} \tag{3.27}$$

Here $\boldsymbol{x_a^t}$, $\boldsymbol{x_b^t}$ and $\boldsymbol{x_c^t}$ are randomly chosen candidate solutions, $\boldsymbol{M}$ is the mutation factor (between 0 and 2) and $\boldsymbol{v}$ is a donor vector. $\boldsymbol{u}$ is the trail vector, $\boldsymbol{r}$ is a random variable between $\mathbf{0}$ and $\mathbf{1}$, $\boldsymbol{I_r}$ is random integer between $\mathbf{0}$ and $\boldsymbol{T}$, and $\boldsymbol{CR}$ is crossover constant. The algorithm can be implemented as given in Algorithm 3.

Algorithm 3 DE to solve for f_τ

Initialize population size (N), iterations K, M and CR.
Initialize candidate population x_1 to x_N randomly.
for $k = 0 : K$ **do**
    for $i = 1 : N$ **do**
        Randomly select x_a, x_b and x_c.
        $v_i \leftarrow x_a + M.(x_b - x_c)$.
        if $r_j \leq CR$ or $j = I_{integer}$ **then**
            $u_i \leftarrow v_i$
        if $r_j > CR$ or $j \neq I_r$ **then**
            $u_i \leftarrow x_i$
        if $F_\tau(u_i) \leq F_\tau(x_i)$ **then**
            $x_i \leftarrow u_i$
Pick x_i with minimum $f_\tau(x_i)$ value

- **DBC Algorithm with Momentum based Gradient Descent:**

  Gradient Descent (GD) is a gradient-based iterative optimization technique. It updates the parameters (in our case $\boldsymbol{\Delta b_t}$) of the objective function by using the slope of the function w.r.t. the parameter. Momentum-based GD (MGD)[55] helps in accelerating the update process by adding a fraction of old update value to the

new one. This also helps in reducing the damping oscillations present within the vanilla gradient descent method. The algorithm can be implemented as given in Algorithm 4. In the algorithm (Algorithm 3), $\boldsymbol{v^k}$ is the velocity vector of the $\boldsymbol{k^{th}}$

Algorithm 4 MGD to solve for f_τ

1: Initialize number of iterations K, learning rate (η) and velocity coefficient (λ)
2: Initialize solution $\Delta b(\Delta b_1, ... \Delta b_T)$ randomly.
3: **for** $k = 0 : K$ **do**
4: **for** $t = \tau : \tau + T$ **do**
5: Calculate $\Delta_{\Delta b_i} F_\tau(\Delta b)$
6: $v_t^k \leftarrow \lambda v_t^{k-1} + \eta \Delta_{\Delta b_i} F_\tau(\Delta b)$
7: $\Delta b_i \leftarrow \Delta b_i - v_t^k$

iteration, $\boldsymbol{\lambda}$ is the momentum coefficient and $\boldsymbol{\eta}$ is the learning rate.

3.4 Experimental Setup

For evaluating the proposed model, all five approaches are tested in various energy trading scenarios. As explained earlier, the proposed DBC algorithm is tested with two optimization algorithms: DE algorithm and MGD. The overall approaches are mentioned as **DBC:DE** and **DBC:GD** in further text. For DE, the population size is taken as **40**, mutation factor as **0.8** and crossover constant as **0.9**. For MGD, the learning rate is iteratively reduced from **0.2** to **0.01** and momentum coefficient is increased from **0.5** to **0.9**.

In the following simulations, the proposed algorithms are tested using the hourly traces of electricity prices ($\boldsymbol{p_t}$), harvested energy ($\boldsymbol{s_t}$) and electricity demand ($\boldsymbol{d_t}$). This was done using three different load profiles (a small scale **Residential** user, a Walmart Super-center as a medium scale **Commercial** user and an automotive assembly unit as a large-scale **Industrial** user) in three different electricity markets (**Ontario**[48], **California**[49], and **New-York**[50]). The data was collected for a one year period from 1/1/2012-12/31/2012. The solar data for these areas was collected from National Solar Radiation Database (NSRDB)[59]. This dataset is based on National renewable energy laboratory (NREL)[60] developed Physical Solar Model (PSM). PSM makes use of various atmospheric properties (gathered by Geostationary Operational Environmental Satellite

data) as input to a radiative transfer model to calculate the surface radiation[61, 62]. This dataset can be used to obtain a solar energy profile for the end-user, assuming the end-user is equipped with solar panels of certain required dimension.

For all the scenarios, to account for the electrical conversion and transmission loss and lower selling price, the parameter $\boldsymbol{\beta}$ while selling the electricity is set to $\mathbf{0.8}$. So, the selling price is taken to be 20% lower than the buying price. As each time slot is of $\mathbf{1hr}$, the value $\boldsymbol{t_f}$ is set to $\mathbf{8760}$ hours. To find a suitable value of the hyper-parameter $\boldsymbol{T}$, the proposed algorithm was tested on different values of $\boldsymbol{T}$ using a smaller data-set of 1 month. It is clear from Figure 3.3 that beyond a certain value of $\boldsymbol{T}$ ($\mathbf{8}$ in this case), the loss starts increasing. This is due to the larger error induced during estimations of $\boldsymbol{p_t}$, $\boldsymbol{d_t}$ and $\boldsymbol{s_t}$ for later time periods. While on the other hand, the lower $\boldsymbol{T}$ value would result in sub-optimal algorithm solutions due to use of the lower number of data slots for prediction of battery charge state.

For simulation purpose, the batteries were considered to be deep cycle batteries. $\boldsymbol{b^{min}}$ was taken to be $\mathbf{20}$% of the battery capacity ($\boldsymbol{b^{capacity}}$). Further, maximum charging rate ($\boldsymbol{db^{crate}}$) and maximum discharging rate ($\boldsymbol{db^{drate}}$) were also considered to be $\mathbf{50}$% of the $\boldsymbol{b^{capacity}}$. These limits were selected as such for the safe operation of the battery. Maximum charging rate ($\boldsymbol{db^{crate}}$) and maximum discharging rate ($\boldsymbol{db^{drate}}$) were selected to limit the number of cycles used by the battery within a particular day.

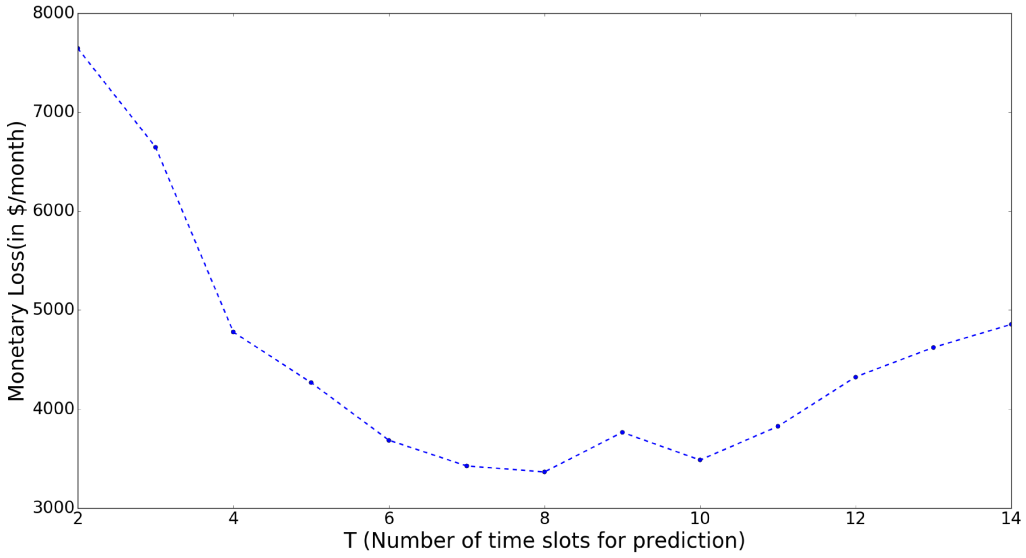

Figure 3.3: Effect of parameter T on DBC algorithm

Table 3.1: Tested Load Profiles

	Unit	Residential	Commercial	Industrial
$\boldsymbol{Net\ Consumption}$	MWh/year	10	5000	75000
$\boldsymbol{PV\ Size}$	kW	4	1000	15000
$\boldsymbol{b^{capacity}}$	kWh	5	2500	37500
$\boldsymbol{b^{min}}$	kWh	1	500	7500
$\boldsymbol{db^{crate}}$	kWh	2.5	1250	18750
$\boldsymbol{db^{drate}}$	kWh	2.5	1250	18750

The residential user was considered to be equipped with solar panels with a total capacity of $\boldsymbol{4kW}$. The annual electricity consumption of the user was around $\boldsymbol{10MWh/year}$. Further, the user is equipped with a battery bank of $\boldsymbol{5kWh}$ total capacity ($\boldsymbol{b^{capacity}}$). For the commercial user case, load profile of an average Walmart Supercenter [63] was considered. For this user, mean annual electricity consumption of $\boldsymbol{5000MWh/year}$ is taken. The unit was considered to be equipped with solar panels of $\boldsymbol{1MW}$ capacity with a total battery capacity of $\boldsymbol{2.5MWh}$. Further, for the industrial load, an automotive assembly unit with an average annual electricity consumption of $\boldsymbol{75000MWh/year}$ is considered. The unit was considered to be equipped with solar panels of $\boldsymbol{15MW}$ capacity with a total battery capacity of $\boldsymbol{37.5MWh}$. Table 3.1 presents the values of all the parameters used in further simulations, related to all three load profiles.

3.5 Simulation Results And Analysis

For simulating the battery dynamics, "Thundersky Winston LiFePO4 Battery" (Model No: WB-LYP1000AHC(A)) were considered. Each battery has a nominal capacity of $\boldsymbol{3kWh}$. These batteries are known to last $\boldsymbol{5000-7000}$ cycles before losing $\boldsymbol{30}$% of its capacity. For this study, the cycle life for the battery system is taken to be $\boldsymbol{6000}$ cycles. The price of each battery is $\boldsymbol{1000}$\$. So, cost per kWh of battery system is $\boldsymbol{350\$/kWh}(=\boldsymbol{1050\$/3kWh})$.

3.5.1 Performance Parameters

To evaluate the simulation results following performance parameters are used:-

- **Loss (L_y in $/year)**: This is the net monetary loss accumulated by the strategy at the end of the year. So, L_y^{ws}, L_y^{greedy}, L_y^{gd}, L_y^{de} and L_y^{rl} represent the loss accumulated at the end of year by using Without Solar, Greedy, DBC:GD, DBC:DE and RL strategy respectively.

- **Profit (p_1 in $/year)**: This is the net monetary profit accumulated by a certain strategy at the end of the year due to use of the PV and battery system. It can be calculated by using Eq.(3.28). Here, i represent the particular strategy (DBC:GD, DBC:DE and RL).

$$p_1^i = L^{ws} - L^i \tag{3.28}$$

  So, p_1^{gd}, p_1^{de} and p_1^{rl} represent the profit accumulated at the end of year by using DBC:GD, DBC:DE and RL strategy respectively.

- **Profit (p_2 in $/year)**: This is the net monetary profit accumulated by a certain strategy at the end of the year due to use of the battery system. It can be calculated by using Eq.(3.29). Here, i represent the particular strategy (DBC:GD, DBC:DE and RL).

$$p_2^i = L^{greedy} - L^i \tag{3.29}$$

  So, p_2^{gd}, p_2^{de} and p_2^{rl} represent the profit accumulated at the end of year by using DBC:GD, DBC:DE and RL strategy respectively.

- **Cycles (c in $cycle/year$)**: This is the net battery charge-discharge cycles used by a strategy (for the purpose of energy trading) by the end of the year. Each cycle is equivalent to one full charge and one full discharge of the battery. So, c^{gd}, c^{de} and c^{rl} represent the cycles used by Without Solar, Greedy, DBC:GD, DBC:DE and RL strategy respectively.

- **Profit per cycle (p_1/c in $/cycle)**: This is the net profit (p_1: by using the PV and battery system) to cycle ratio of a particular strategy.

- **Profit per cycle (p_2/c in $/cycle)**: This is the net profit (p_2: by using the battery system) to cycle ratio of a particular strategy.

- **Revenue (in $)**: This represent the net revenue generated by the battery during its lifetime. It can be calculated by using Eq.(3.30). Here, **6000** represent the cycle

life of the battery.

$$Revenue^i = (p_2^i/c^i) * 6000 \tag{3.30}$$

- **Gross Profit (GP in \$)**: This represent the gross profit generated by the battery during its lifetime. It can be calculated by deducting cost of the battery system from the revenue (Eq.(3.31)).

$$GP^i = Revenue^i - cost \tag{3.31}$$

- **% Gross Profit (%GP in %)**: This represent the percentage of profit due to investment in battery system. It can be calculated as shown in (Eq.(3.32)).

$$\%GP^i = 100 * \frac{Revenue^i - cost}{cost} \tag{3.32}$$

- **Lifetime (in *years*)**: This represents the lifetime of the battery system in years by using a particular strategy. After that, the battery cells are required to be replaced. It can be calculated as shown in (Eq.(3.33)). Here, **6000** represent the cycle life of the battery.

$$Lifetime^i = 6000/c^i \tag{3.33}$$

3.5.2 Simulation Results

The simulation results for the **9** load profiles are shown below:-

- **Case 1: Ontario Residential Case:** In this case, the net cost of the battery system is $\mathbf{1750}\$(= \mathbf{0.35}\$/\boldsymbol{kWh} * \mathbf{5}\boldsymbol{kWh})$. Figure 3.4 shows the loss accumulated by the residential user up to each time slot of the year, in the Ontario state. Different colored lines are used to represent the performance of the different trading strategies. In this case, the order of monetary loss from higher to lower is: DBC:DE > DBC:GD > RL > Greedy. DBC:DE easily outperformed all other approaches. Figure 3.5 shows the cumulative profit generated by the end-user due to use of battery system for 3 different trading strategies: DBC:GD, DBC:DE and RL. Essentially, its the profit accumulated compared to the greedy trading strategy. For this case the $\boldsymbol{L_y^{ws}}$, $\boldsymbol{L_y^{greedy}}$, $\boldsymbol{L_y^{gd}}$, $\boldsymbol{L_y^{de}}$ and $\boldsymbol{L_y^{rl}}$ were found out to be $\mathbf{347.18}\$/\boldsymbol{year}$, $\mathbf{156.95}\$/\boldsymbol{year}$, $\mathbf{109.33}\$/\boldsymbol{year}$, $\mathbf{6.95}\$/\boldsymbol{year}$ and $\mathbf{112.75}\$/\boldsymbol{year}$ respectively. Table 3.2 summarizes the performance parameters for this case. Clearly the DBC:DE

performed the best in this scenario by generating a profit of around **21.99**% in the battery lifetime.

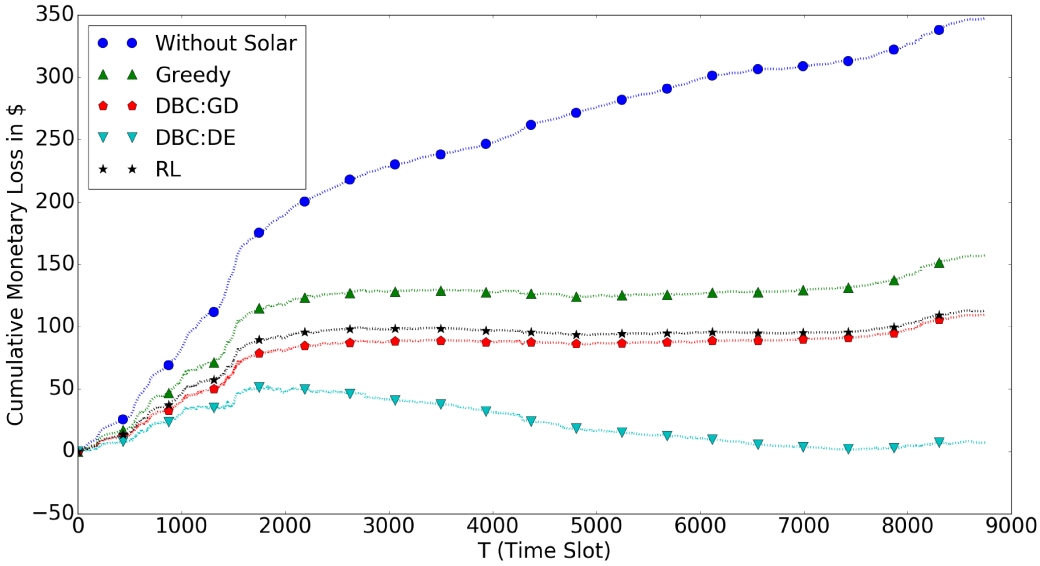

Figure 3.4: Ontario Residential Case: Cumulative loss curve

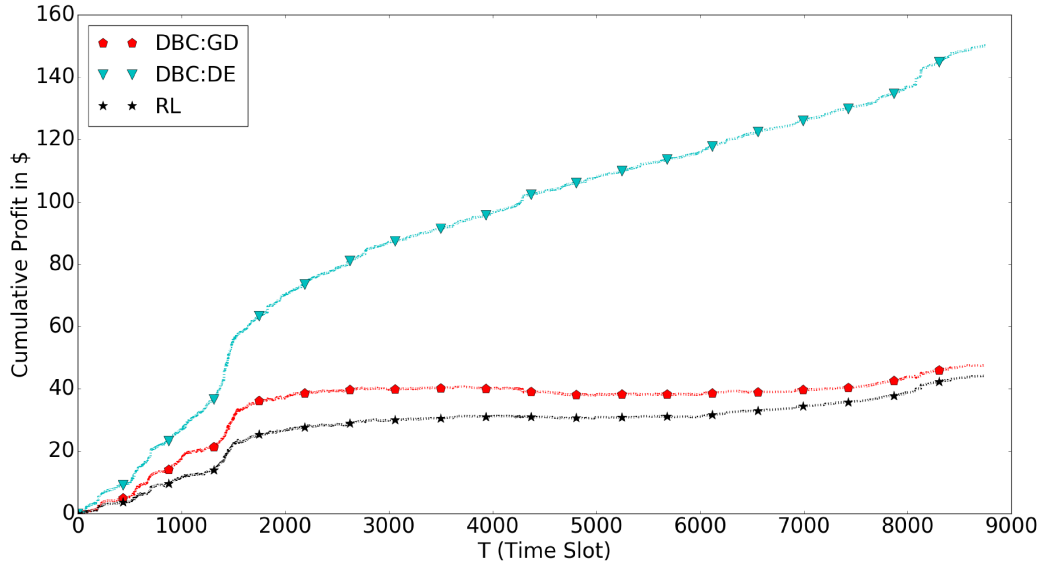

Figure 3.5: Ontario Residential Case: Cumulative Profit by using Battery system

- **Case 2: Ontario Commercial Case:** In this case, the net cost of the battery system is **875000**$(= **0.35**$/$\boldsymbol{kWh} * \mathbf{2500}\boldsymbol{kWh}$). Figure 3.6 shows the loss accumulated by the Commercial user up to each time slot of the year, in the Ontario state. Different colored lines are used to represent the performance of the different

Table 3.2: Ontario Residential Case: Performance Parameters

Parameter	Unit	DBC:GD	DBC:DE	RL
Loss (L_y)	\$/year	109.33	6.95	112.75
Profit (p_1)	\$/year	237.84	340.23	234.43
Profit (p_2)	\$/year	47.62	150.00	44.20
Cycles (c)	cycle/year	381.26	421.60	391.34
p_1/c	\$/cycle	0.62	0.81	0.60
p_2/c	\$/cycle	0.12	0.36	0.11
Revenue	\$	749.41	2134.74	677.70
Gross Profit(GP)	\$	-1000.59	384.74	-1072.30
% Gross Profit$(\%GP)$	%	-57.18	21.99	-61.27
Lifetime	years	15.74	14.23	15.33

trading strategies. The order of monetary loss from higher to lower is: DBC:DE > RL > DBC:GD > Greedy. Overall, DBC:DE gave better returns closely followed by the RL strategy. Figure 3.7 shows the cumulative profit generated by the end-user due to use of battery system for DBC:GD, DBC:DE and RL trading strategies. For this case the $\boldsymbol{L_y^{ws}}$, $\boldsymbol{L_y^{greedy}}$, $\boldsymbol{L_y^{gd}}$, $\boldsymbol{L_y^{de}}$ and $\boldsymbol{L_y^{rl}}$ were found out to be $\mathbf{161786.81\$/year}$, $\mathbf{110771.45\$/year}$, $\mathbf{79928.21\$/year}$, $\mathbf{37238.80\$/year}$ and $\mathbf{48732.89\$/year}$ respectively. Table 3.3 summarizes the performance parameters for the Ontario Commercial case. Both DBC:DE and RL strategy were able to generate positive overall returns during battery lifetime with DBC:DE giving a $\mathbf{25.43}\%$ gross profit and RL giving $\mathbf{8.41}\%$ gross profit.

- **Case 3: Ontario Industrial Case:** In this case, the net cost of the battery system is $\mathbf{13125000\$(= 0.35\$/kWh * 37500kWh)}$. Figure 3.8 shows the loss accumulated by the Industrial user up to each time slot of the year, in the Ontario state. Different colored lines are used to represent the performance of the different trading strategies. The order of monetary loss from higher to lower is: DBC:DE > RL > DBC:GD > Greedy. DBC:DE easily outperformed all other approaches in this case. Figure 3.9 shows the cumulative profit generated by the end-user due to use of battery system for DBC:GD, DBC:DE and RL trading strategies. For this

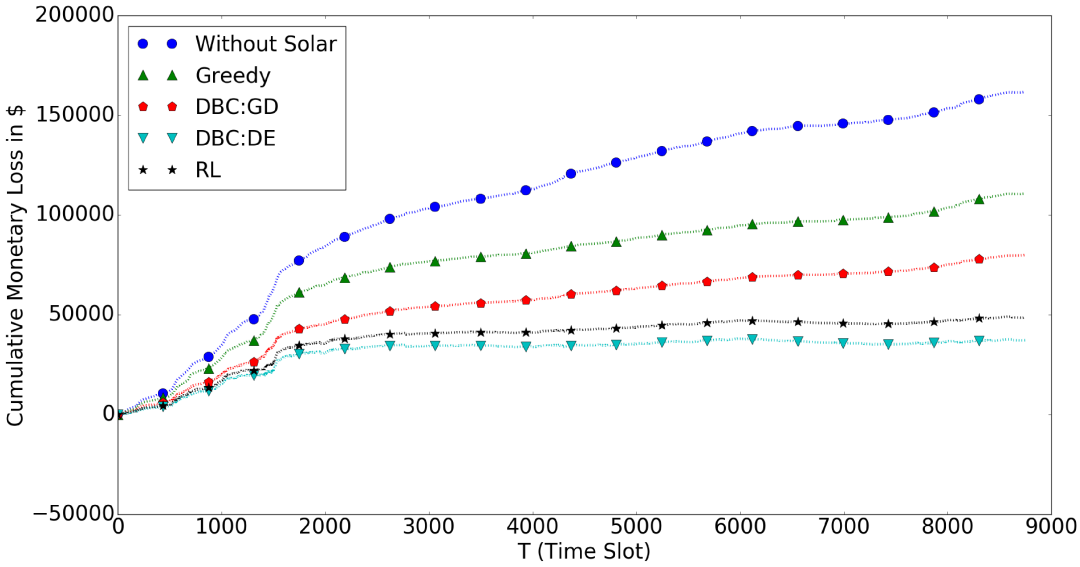

Figure 3.6: Ontario Commercial Case: Cumulative loss curve

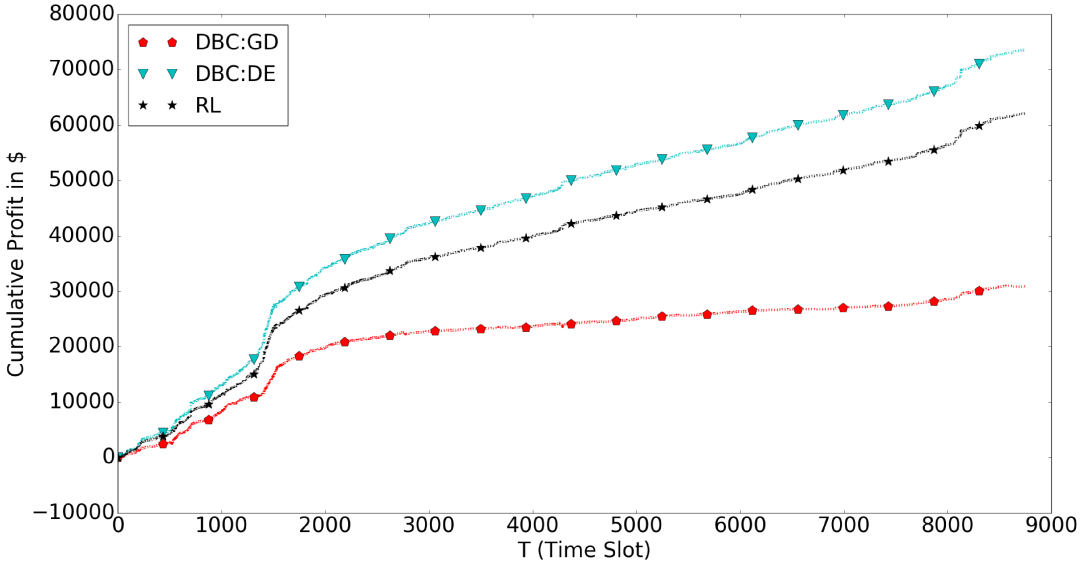

Figure 3.7: Ontario Commercial Case: Cumulative Profit by using Battery system

Table 3.3: Ontario Commercial Case: Performance Parameters

Parameter	Unit	DBC:GD	DBC:DE	RL
Loss (L_y)	\$/year	79928.21	37238.80	48732.89
Profit (p_1)	\$/year	81858.60	124548.00	113053.92
Profit (p_2)	\$/year	30843.24	73532.65	62038.57
Cycles (c)	cycle/year	389.22	402.01	392.42
p_1/c	\$/cycle	210.31	309.81	288.09
p_2/c	\$/cycle	79.24	182.91	158.09
Revenue	\$	475458.75	1097469.95	948553.18
Gross Profit(GP)	\$	-399541.25	222469.95	73553.18
% Gross Profit$(\%GP)$	%	-45.66	25.43	8.41
Lifetime	years	15.42	14.92	15.29

case the $\boldsymbol{L_y^{ws}}$, $\boldsymbol{L_y^{greedy}}$, $\boldsymbol{L_y^{gd}}$, $\boldsymbol{L_y^{de}}$ and $\boldsymbol{L_y^{rl}}$ were found out to be **2430605.69**\$/***year***, **1664863.18**\$/***year***, **1198308.72**\$/***year***, **561225.13**\$/***year*** and **894665.05**\$/***year*** respectively. Table 3.4 summarizes the performance parameters for this case. Clearly the DBC:DE performed the best in this scenario by generating a gross profit of around **25.64**% in the battery lifetime.

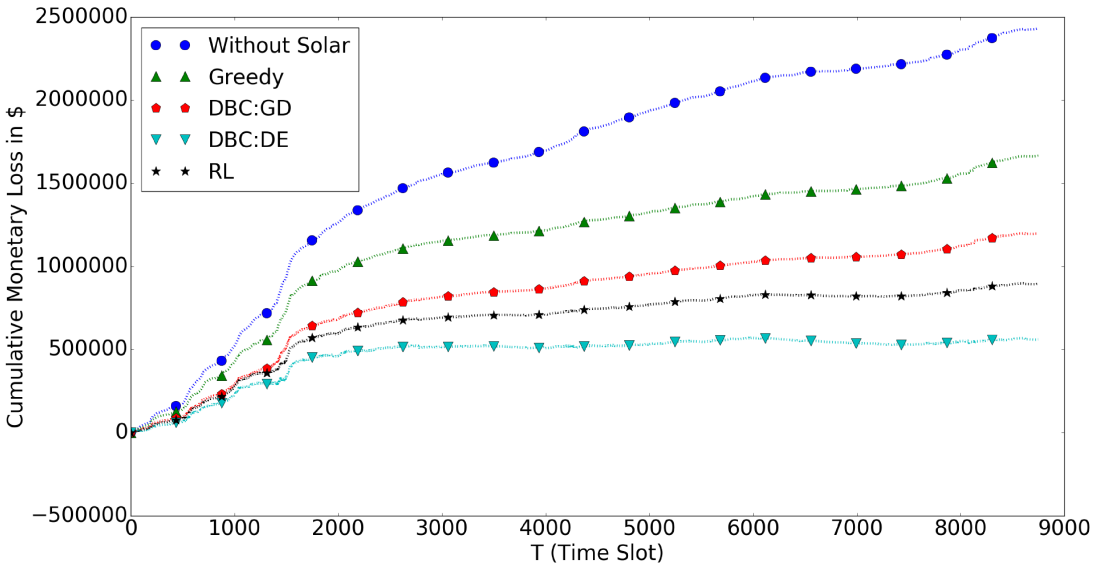

Figure 3.8: Ontario Industrial Case: Cumulative loss curve

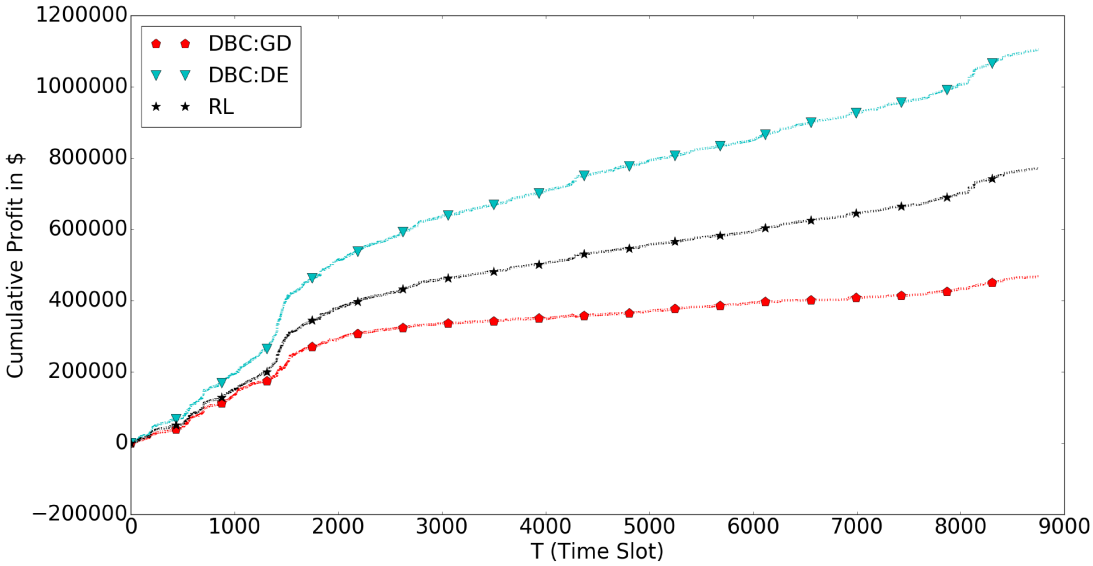

Figure 3.9: Ontario Industrial Case: Cumulative Profit by using Battery system

Table 3.4: Ontario Industrial Case: Performance Parameters

Parameter	**Unit**	**DBC:GD**	**DBC:DE**	**RL**
Loss (L_y)	\$/year	1198308.72	561225.13	894665.05
Profit (p_1)	\$/year	1232296.97	1869380.56	1535940.65
Profit (p_2)	\$/year	466554.45	1103638.05	770198.13
Cycles (c)	cycle/year	388.44	401.55	391.71
p_1/c	\$/cycle	3172.47	4655.40	3921.08
p_2/c	\$/cycle	1201.11	2748.44	1966.23
Revenue	\$	7206677.78	16490632.58	11797352.33
Gross Profit (GP)	\$	-5918322.22	3365632.58	-1327647.67
% ***Gross Profit*** $(\%GP)$	%	-45.09	25.64	-10.12
Lifetime	years	15.45	14.94	15.32

- **Case 4: California Residential Case:** In this case, the net cost of the battery system is $\mathbf{1750\$(= 0.35\$/kWh * 5kWh)}$. Figure 3.10 shows the loss accumulated by the Residential user up to each time slot of the year, in the California state. Different colored lines are used to represent the performance of the different trading strategies. The order of monetary loss from higher to lower is: DBC:DE > RL > DBC:GD > Greedy. DBC:DE easily outperformed all other approaches in this case. Figure 3.11 shows the cumulative profit generated by the end-user due to use of battery system for 3 different trading strategies: DBC:GD, DBC:DE and RL. In this case, the $\boldsymbol{L_y^{ws}}$, $\boldsymbol{L_y^{greedy}}$, $\boldsymbol{L_y^{gd}}$, $\boldsymbol{L_y^{de}}$ and $\boldsymbol{L_y^{rl}}$ were found out to be $\mathbf{308.25\$/year}$, $\mathbf{51.32\$/year}$, $\mathbf{42.21\$/year}$, $\mathbf{-45.19\$/year}$ and $\mathbf{13.07\$/year}$ respectively. Negative cumulative loss value of DBC:DE trading strategy ($\boldsymbol{L^{de}}$) suggests that in this case the end-user was paid more money for selling the electricity than it had to pay for buying electricity from the grid. Table 3.5 summarizes the performance parameters for this case. Clearly the DBC:DE performed the best in this case. It generated a gross profit of around $\mathbf{1.79\%}$ in the battery lifetime.

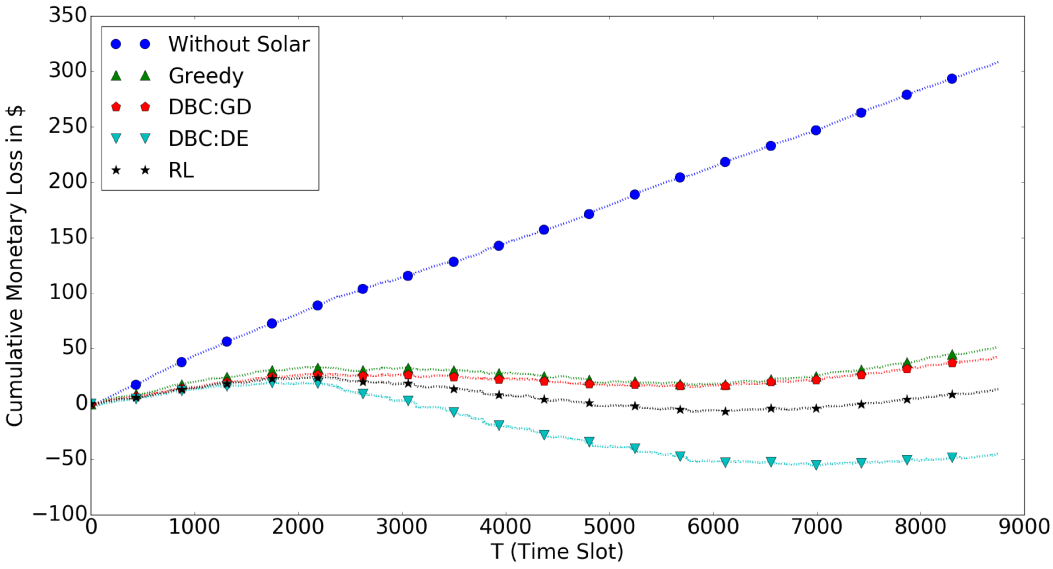

Figure 3.10: California Residential Case: Cumulative loss curve

- **Case 5: California Commercial Case:** In this case, the net cost of the battery system is $\mathbf{875000\$(= 0.35\$/kWh * 2500kWh)}$. Figure 3.12 shows the loss accumulated by the Commercial user up to each time slot of the year, in the California state. Different colored lines are used to represent the performance of the

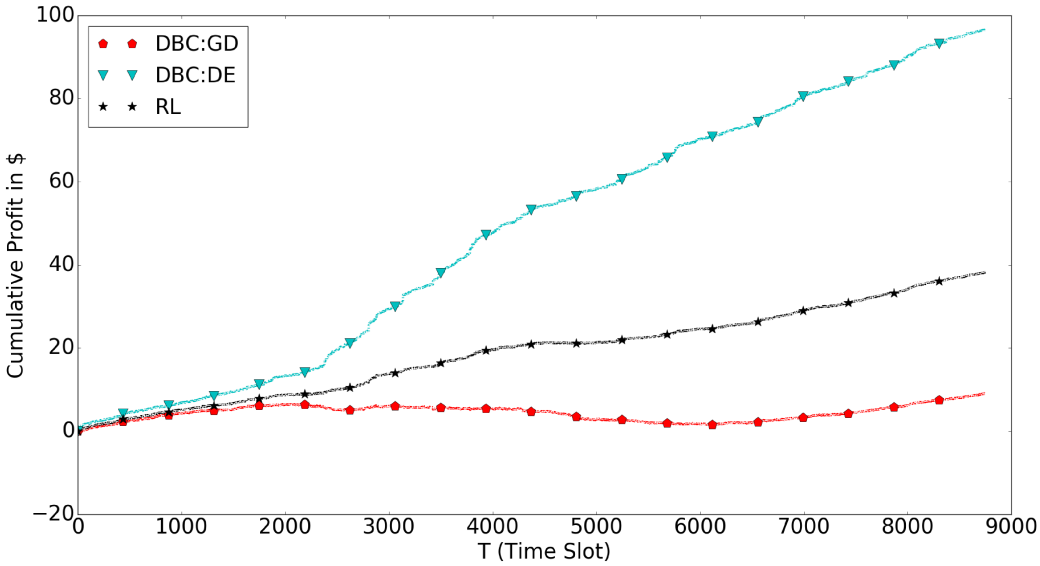

Figure 3.11: California Residential Case: Cumulative Profit by using Battery system

Table 3.5: California Residential Case: Performance Parameters

Parameter	**Unit**	**DBC:GD**	**DBC:DE**	**RL**
Loss (L_y)	\$/year	42.21	-45.19	13.08
Profit (p_1)	\$/year	266.04	353.44	295.17
Profit (p_2)	\$/year	9.11	96.51	38.24
Cycles (c)	cycle/year	331.74	325.09	330.08
p_1/c	\$/cycle	0.80	1.09	0.89
p_2/c	\$/cycle	0.03	0.30	0.12
Revenue	\$	164.78	1781.24	695.20
Gross Profit (GP)	\$	-1585.22	31.24	-1054.80
% ***Gross Profit*** $(\%GP)$	%	-90.58	1.79	-60.27
Lifetime	years	18.09	18.46	18.18

different trading strategies. The order of monetary loss from higher to lower is: DBC:DE > RL > DBC:GD > Greedy. Clearly, the DBC:DE outperformed all other approaches in this case. Figure 3.13 shows the cumulative profit generated by the end-user due to use of battery system for DBC:GD, DBC:DE and RL trading strategies. For this case the $\boldsymbol{L_y^{ws}}$, $\boldsymbol{L_y^{greedy}}$, $\boldsymbol{L_y^{gd}}$, $\boldsymbol{L_y^{de}}$ and $\boldsymbol{L_y^{rl}}$ were found out to be $\mathbf{150489.90\$/year}$, $\mathbf{81010.28\$/year}$, $\mathbf{65171.16\$/year}$, $\mathbf{34929.56\$/year}$ and $\mathbf{56137.95\$/year}$ respectively. Table 3.6 summarizes the performance parameters for the California Commercial case. Clearly, the DBC:DE outperformed all other strategies by generating a gross profit of around **8.28%** in the battery lifetime.

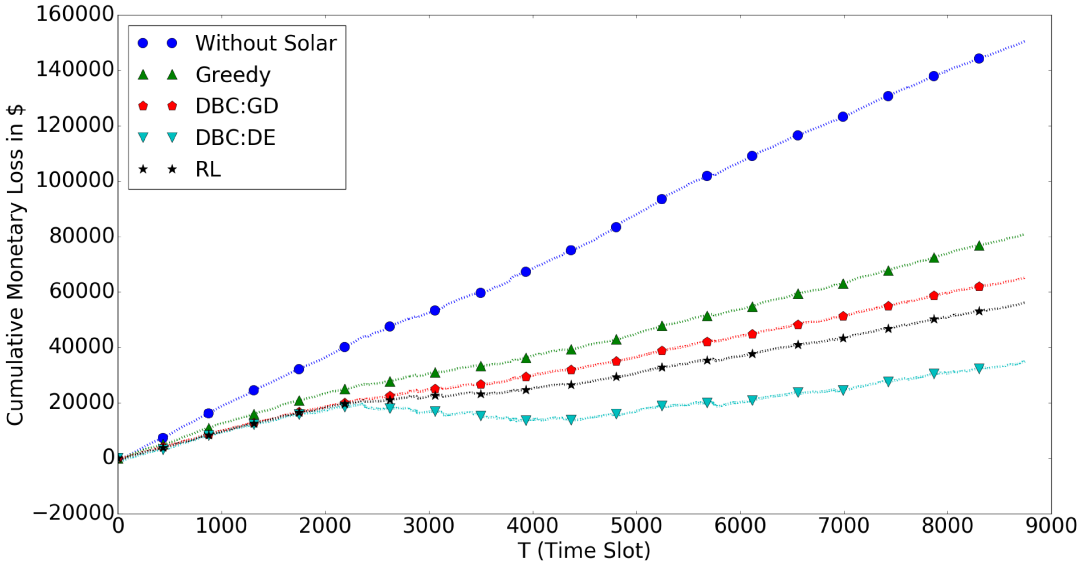

Figure 3.12: California Commercial Case: Cumulative loss curve

- **Case 6: California Industrial Case:** In this case, the net cost of the battery system is $\mathbf{13125000\$(= 0.35\$/kWh * 37500kWh)}$. Figure 3.14 shows the loss accumulated by the Industrial user up to each time slot of the year, in the California state. Different colored lines are used to represent the performance of the different trading strategies. The order of monetary loss from higher to lower is: DBC:DE > RL > DBC:GD > Greedy. DBC:DE outperformed all other approaches in this case. Figure 3.15 shows the cumulative profit generated by the end-user due to use of battery system for DBC:GD, DBC:DE and RL trading strategies. For this case the $\boldsymbol{L_y^{ws}}$, $\boldsymbol{L_y^{greedy}}$, $\boldsymbol{L_y^{gd}}$, $\boldsymbol{L_y^{de}}$ and $\boldsymbol{L_y^{rl}}$ were found out to be $\mathbf{2257832.63\$/year}$, $\mathbf{1215076.38\$/year}$, $\mathbf{995202.66\$/year}$, $\mathbf{524404.64\$/year}$ and $\mathbf{838269.99\$/year}$

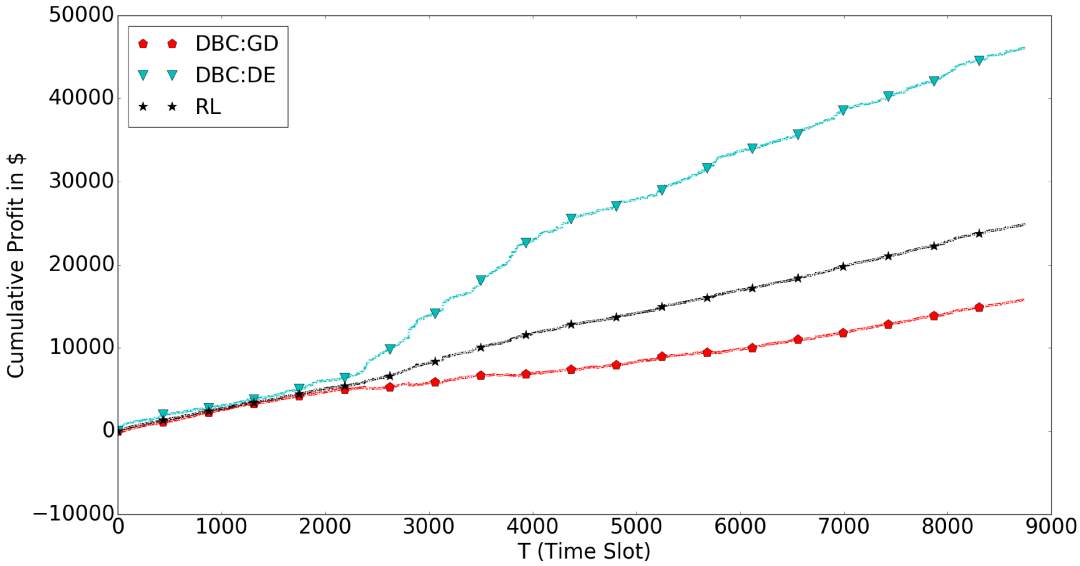

Figure 3.13: California Commercial Case: Cumulative Profit by using Battery system

Table 3.6: California Commercial Case: Performance Parameters

Parameter	**Unit**	**DBC:GD**	**DBC:DE**	**RL**
Loss (L_y)	\$/year	65171.16	34929.56	56137.95
Profit (p_1)	\$/year	85318.75	115560.34	94351.95
Profit (p_2)	\$/year	15839.12	46080.71	24872.32
Cycles (c)	cycle/year	334.26	291.81	323.65
p_1/c	\$/cycle	255.25	396.01	291.53
p_2/c	\$/cycle	47.39	157.91	76.85
Revenue	\$	284313.21	947472.89	461098.70
Gross Profit (GP)	\$	-590686.79	72472.89	-413901.30
% ***Gross Profit*** $(\%GP)$	%	-67.51	8.28	-47.30
Lifetime	years	17.95	20.56	18.54

respectively. Table 3.7 summarizes the performance parameters for this case. Clearly the DBC:DE performed the best in this scenario by generating a profit of around **8.43%** in the battery lifetime.

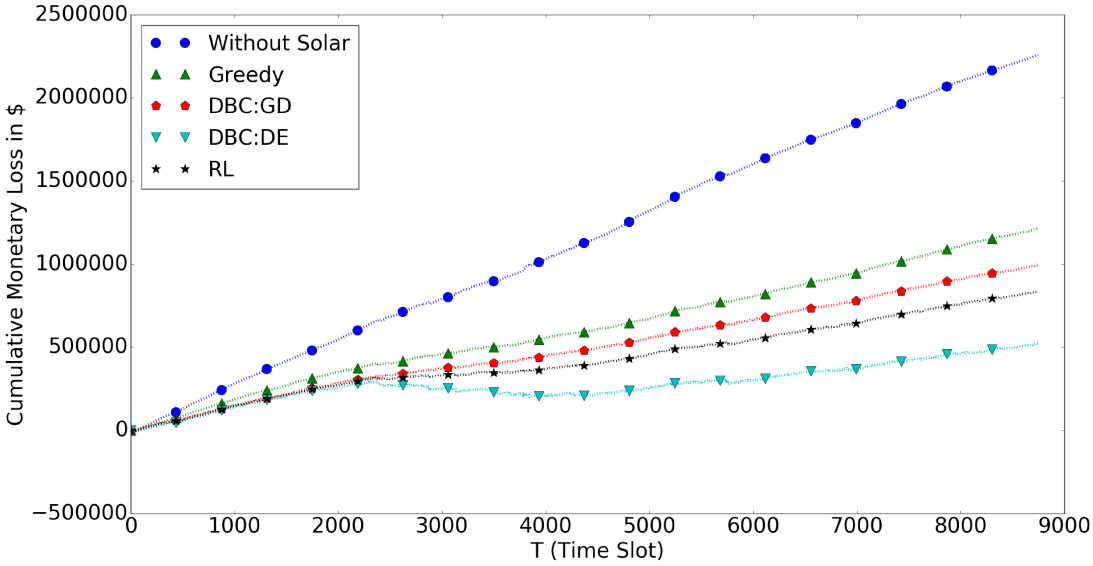

Figure 3.14: California Industrial Case: Cumulative loss curve

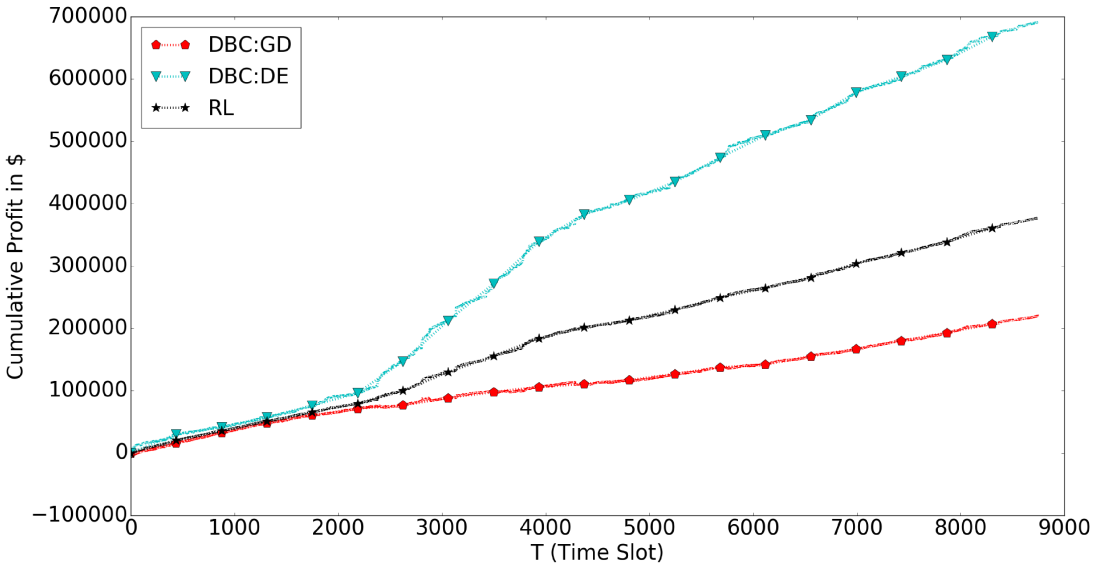

Figure 3.15: California Industrial Case: Cumulative Profit by using Battery system

- **Case 7: New-York Residential Case:** In this case, the net cost of the battery system is $\mathbf{1750\$(= 0.35\$/kWh * 5kWh)}$. Figure 3.16 shows the loss accumulated by the New-York based Residential end-user up to each time slot of the year.

Table 3.7: California Industrial Case: Performance Parameters

Parameter	Unit	DBC:GD	DBC:DE	RL
Loss (L_y)	\$/year	995202.66	524404.64	838269.99
Profit (p_1)	\$/year	1262629.97	1733427.99	1419562.64
Profit (p_2)	\$/year	219873.72	690671.74	376806.40
Cycles (c)	cycle/year	337.21	291.19	325.70
p_1/c	\$/cycle	3744.35	5953.00	4358.45
p_2/c	\$/cycle	652.04	2371.93	1156.90
Revenue	\$	3912236.40	14231584.25	6941404.37
Gross Profit (GP)	\$	-9212763.60	1106584.25	-6183595.63
% ***Gross Profit*** $(\%GP)$	%	-70.19	8.43	-47.11
Lifetime	years	17.79	20.61	18.42

Different colored lines are used to represent the performance of the different trading strategies. The order of monetary loss from higher to lower is: DBC:DE > RL > DBC:GD > Greedy. DBC:DE easily outperformed all other approaches in this case. Figure 3.17 shows the cumulative profit generated by the end-user due to use of battery system for DBC:GD, DBC:DE and RL trading strategies. In this case the $\boldsymbol{L_y^{ws}}$, $\boldsymbol{L_y^{greedy}}$, $\boldsymbol{L_y^{gd}}$, $\boldsymbol{L_y^{de}}$ and $\boldsymbol{L_y^{rl}}$ were found out to be $\mathbf{357.41\$/year}$, $\mathbf{118.76\$/year}$, $\mathbf{89.16\$/year}$, $\mathbf{16.33\$/year}$ and $\mathbf{66.11\$/year}$ respectively. Table 3.8 summarizes the performance parameters for this case. Clearly, the DBC:DE outperformed all other strategies by generating a gross profit of around $\mathbf{11.41\%}$ in the battery lifetime.

- **Case 8: New-York Commercial Case:** In this case, the net cost of the battery system is $\mathbf{875000\$(= 0.35\$/kWh * 2500kWh)}$. Figure 3.18 shows the loss accumulated by the Commercial user up to each time slot of the year, in the New-York state. Different colored lines are used to represent the performance of the different trading strategies. The order of monetary loss from higher to lower is: DBC:DE > RL > DBC:GD > Greedy. DBC:DE strategy clearly outperformed all other approaches in this case. Figure 3.19 shows the cumulative profit generated by the end-user due to use of battery system for DBC:GD, DBC:DE and RL trading

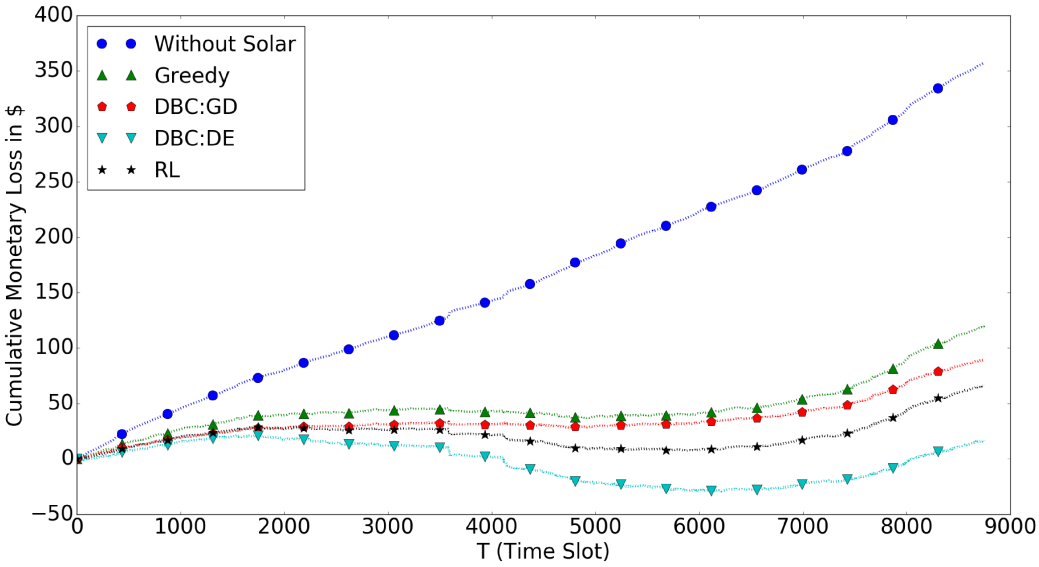

Figure 3.16: New-York Residential Case: Cumulative loss curve

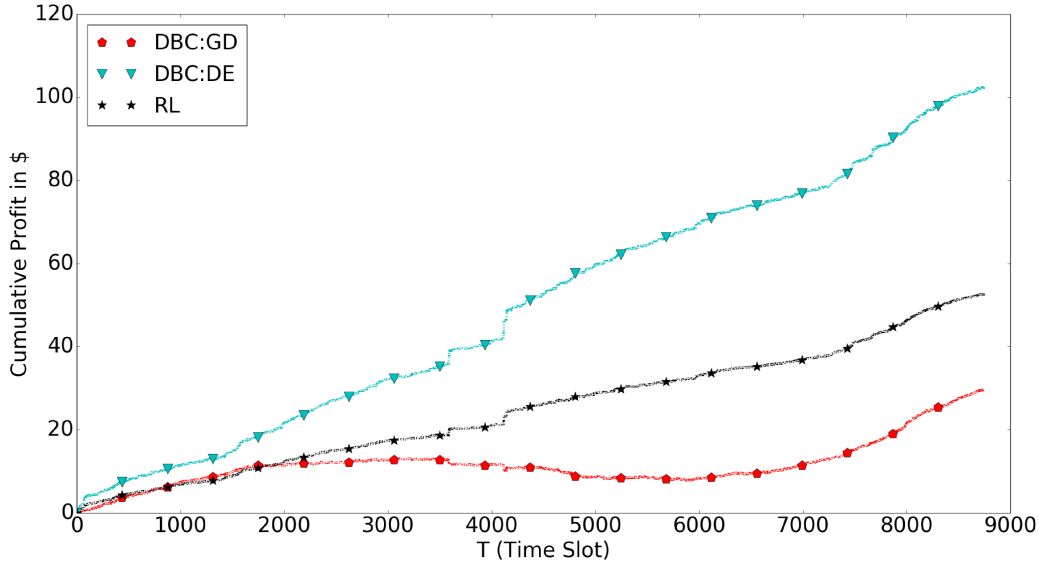

Figure 3.17: New-York Residential Case: Cumulative Profit by using Battery system

Table 3.8: New-York Residential Case: Performance Parameters

Parameter	Unit	DBC:GD	DBC:DE	RL
Loss (L_y)	\$/year	89.16	16.33	66.11
Profit (p_1)	\$/year	268.25	341.08	291.30
Profit (p_2)	\$/year	29.60	102.43	52.65
Cycles (c)	cycle/year	331.80	315.22	327.66
p_1/c	\$/cycle	0.81	1.08	0.89
p_2/c	\$/cycle	0.09	0.32	0.16
Revenue	\$	535.24	1949.72	964.14
Gross Profit (GP)	\$	-1214.76	199.72	-785.86
% ***Gross Profit*** $(\%GP)$	%	-69.41	11.41	-44.91
Lifetime	years	18.08	19.03	18.31

strategies. For this case the $\boldsymbol{L_y^{ws}}$, $\boldsymbol{L_y^{greedy}}$, $\boldsymbol{L_y^{gd}}$, $\boldsymbol{L_y^{de}}$ and $\boldsymbol{L_y^{rl}}$ were found out to be **173884.11**\$/***year***, **109695.46**\$/***year***, **87803.78**\$/***year***, **60179.91**\$/***year*** and **71229.46**\$/***year*** respectively. Table 3.9 summarizes the performance parameters for this case. Clearly, the DBC:DE performed the best in this scenario by generating a profit of around **16.28**% in the battery lifetime.

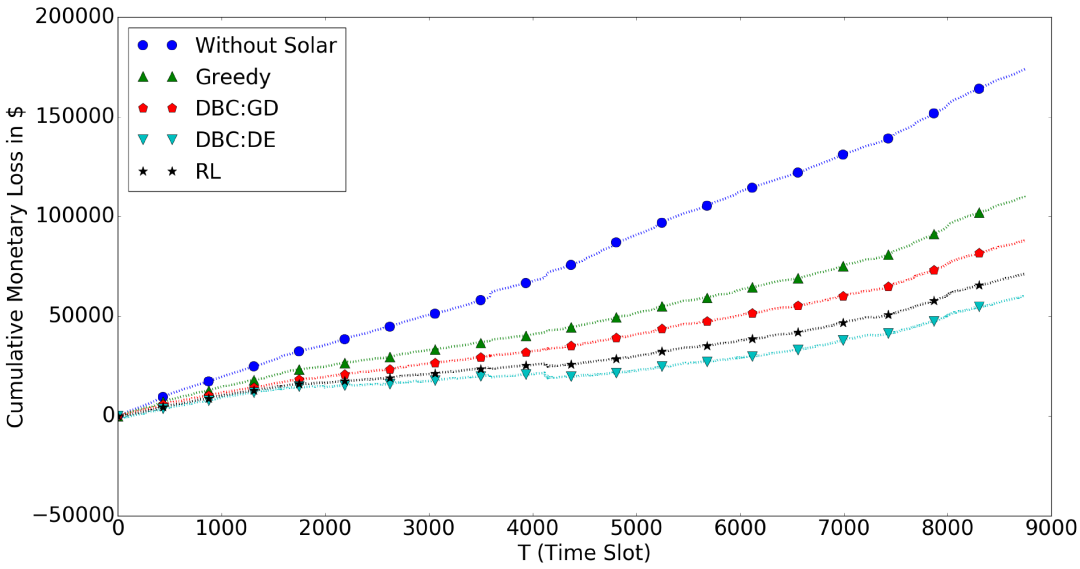

Figure 3.18: New-York Commercial Case: Cumulative loss curve

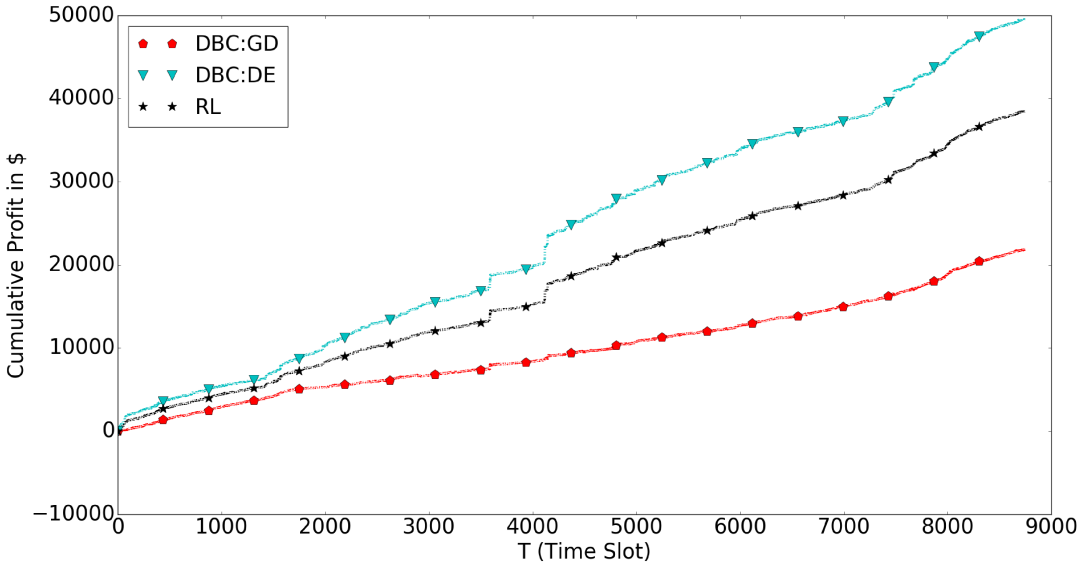

Figure 3.19: New-York Commercial Case: Cumulative Profit by using Battery system

Table 3.9: New-York Commercial Case: Performance Parameters

Parameter	**Unit**	**DBC:GD**	**DBC:DE**	**RL**
Loss (L_y)	\$/year	87803.78	60179.91	71229.46
Profit (p_1)	\$/year	86080.32	113704.20	102654.65
Profit (p_2)	\$/year	21891.67	49515.55	38466.00
Cycles (c)	cycle/year	336.05	291.99	325.04
p_1/c	\$/cycle	256.15	389.42	315.82
p_2/c	\$/cycle	65.14	169.58	118.34
Revenue	\$	390860.03	1017493.29	710061.07
Gross Profit (GP)	\$	-484139.97	142493.29	-164938.93
% ***Gross Profit*** $(\%GP)$	%	-55.33	16.28	-18.85
Lifetime	years	17.85	20.55	18.46

- **Case 9: New-York Industrial Case:** In this case, the net cost of the battery system is $\mathbf{13125000\$(= 0.35\$/kWh * 37500kWh)}$. Figure 3.20 shows the loss accumulated by the New-York based Industrial end-user up to each time slot of the year. Different colored lines are used to represent the performance of the different trading strategies. The order of monetary loss from higher to lower is: DBC:DE > RL > DBC:GD > Greedy. DBC:DE strategy clearly outperformed all other approaches in this case. Figure 3.21 shows the cumulative profit generated by the end-user due to use of battery system for DBC:GD, DBC:DE and RL trading strategies. In this case, the $\boldsymbol{L_y^{ws}}$, $\boldsymbol{L_y^{greedy}}$, $\boldsymbol{L_y^{gd}}$, $\boldsymbol{L_y^{de}}$ and $\boldsymbol{L_y^{rl}}$ were found out to be $\mathbf{2611876.56\$/year}$, $\mathbf{1648640.87\$/year}$, $\mathbf{1223615.89\$/year}$, $\mathbf{905617.21\$/year}$ and $\mathbf{1223452.73\$/year}$ respectively. Table 3.10 summarizes the performance parameters for the New-York Industrial case. Clearly, the DBC:DE outperformed all other strategies by generating a gross profit of around $\mathbf{16.57\%}$ in the battery lifetime.

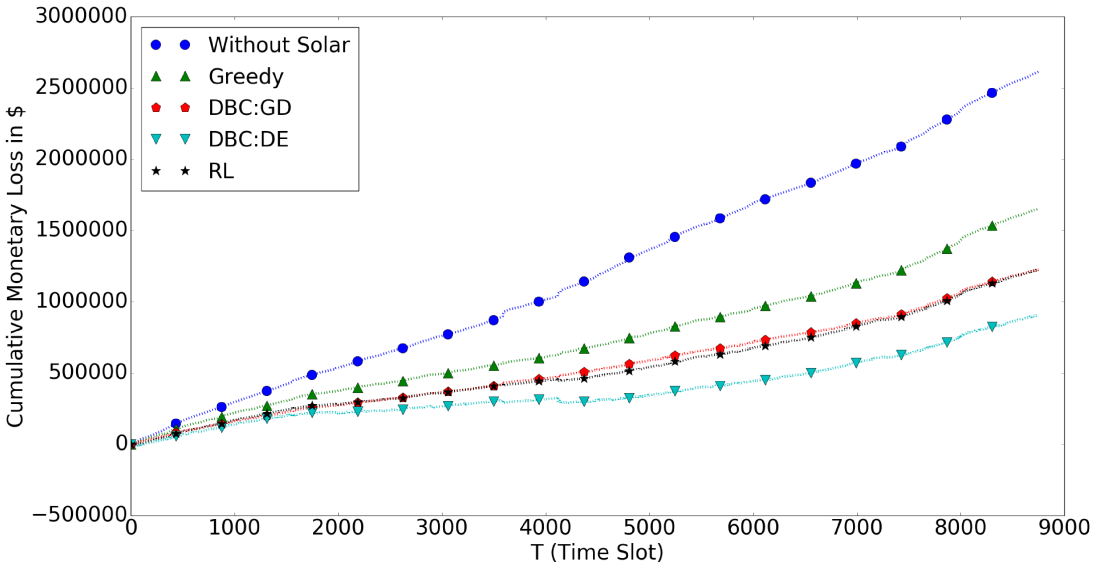

Figure 3.20: New-York Industrial Case: Cumulative loss curve

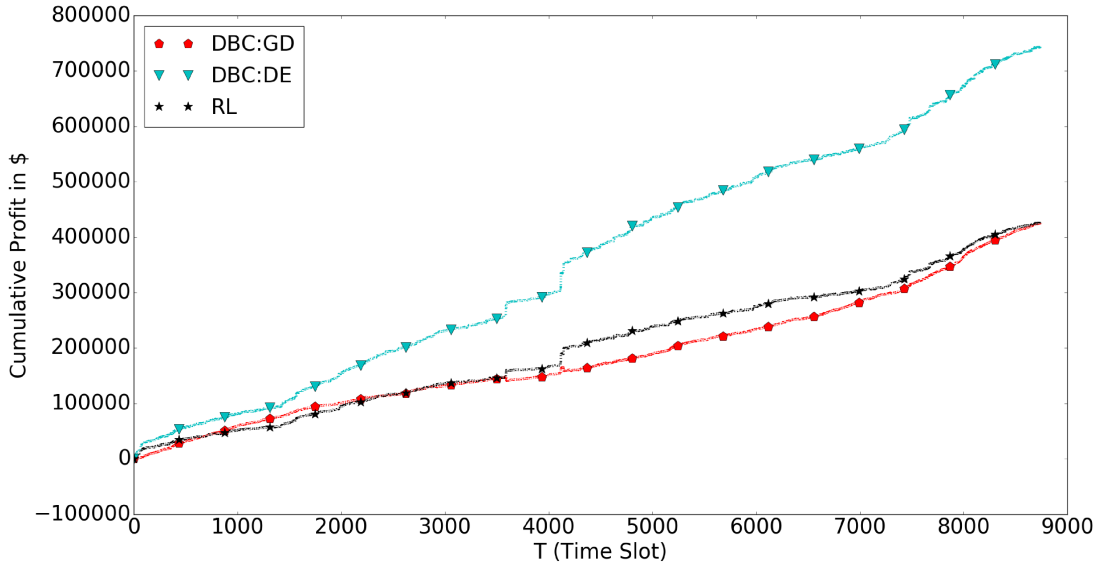

Figure 3.21: New-York Industrial Case: Cumulative Profit by using Battery system

Table 3.10: New-York Industrial Case: Performance Parameters

Parameter	**Unit**	**DBC:GD**	**DBC:DE**	**RL**
Loss (L_y)	\$/year	1223615.89	905617.21	1223452.73
Profit (p_1)	\$/year	1388260.67	1706259.34	1388423.82
Profit (p_2)	\$/year	425024.99	743023.66	425188.14
Cycles (c)	cycle/year	330.90	291.39	321.03
p_1/c	\$/cycle	4195.36	5855.53	4324.96
p_2/c	\$/cycle	1284.44	2549.90	1324.47
Revenue	\$	7706616.93	15299429.65	7946795.02
Gross Profit (GP)	\$	-5418383.07	2174429.65	-5178204.98
% ***Gross Profit*** $(\%GP)$	%	-41.28	16.57	-39.45
Lifetime	years	18.13	20.59	18.69

3.5.3 Performance Analysis

Clearly, the DBC:DE strategy outperformed other methods in all the tested scenarios. In general, the order of monetary loss from higher to lower turned out to be DBC:DE > RL > DBC:GD > Greedy (Except in Ontario Residential case where DBC:GD performed better than RL approach). In all the tested cases, the cumulative loss up to each time slot was minimum for DBC:DE strategy. This is evident from the fact that green line representing DBC:DE algorithm (in Figure 3.4, 3.6, 3.8, 3.10, 3.12, 3.14, 3.16, 3.18, 3.20) is always below all the other lines.

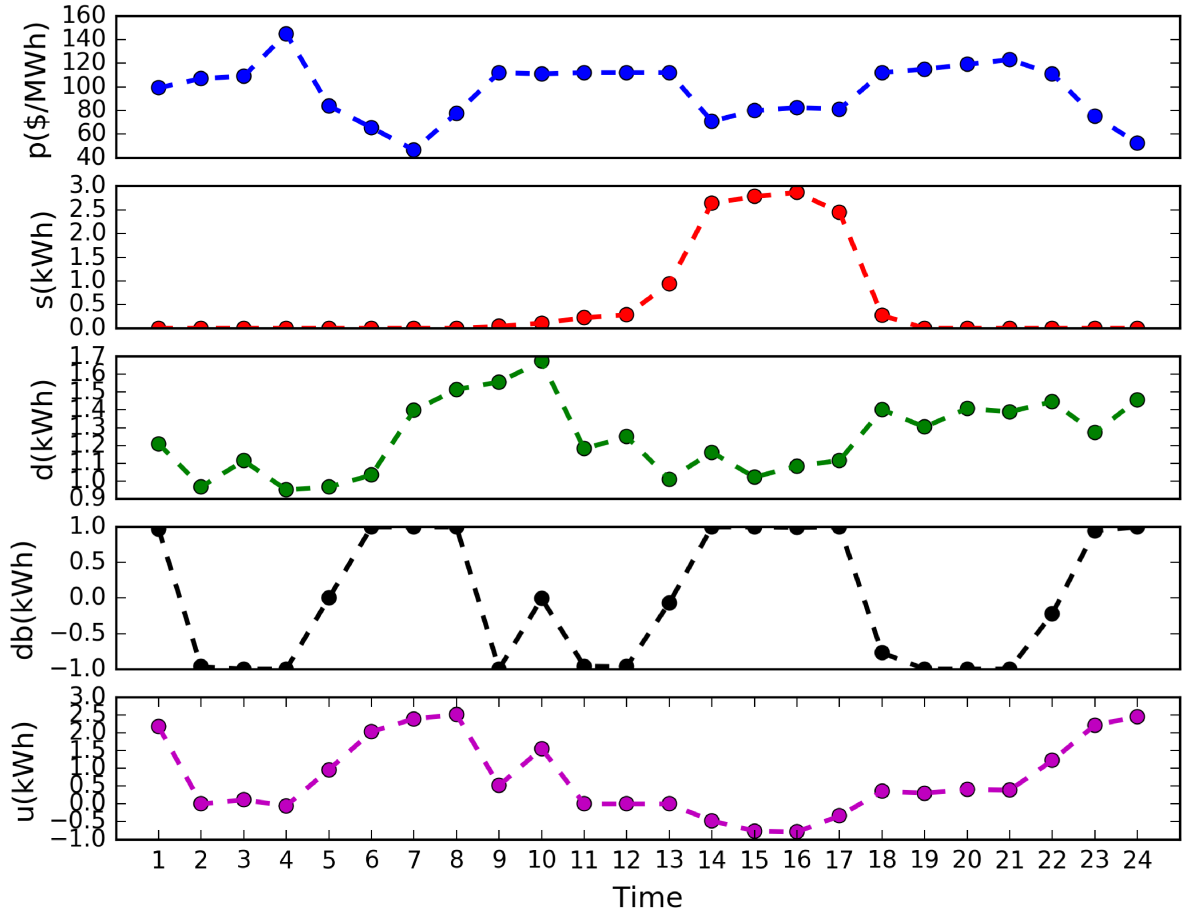

Figure 3.22: DBC:DE decision pattern in Ontario Residential Case

Figure 3.22 shows the proposed algorithm's decision-making pattern for a particular day. The plot shows the change pattern in energy traded ($\boldsymbol{u}$) and change in battery charge ($\boldsymbol{\Delta b}$) w.r.t. changes in market price ($\boldsymbol{p}$), solar power generation ($\boldsymbol{s}$) and load demand ($\boldsymbol{d}$) in a set of 24 consecutive time-slots. The changes in energy traded ($\boldsymbol{u}$) and battery state ($\boldsymbol{b}$) represent the decision-making process of the tested algorithm. Clearly, the time slots

with decreased electricity prices are followed by a positive $\boldsymbol{u}$ value representing that the energy was bought during those time slots. Similarly, for time slots with high electricity prices the energy was sold to the grid represented by its negative values in those time slots. Further, during time slots with high solar power generation the battery is getting charged (represented by positive $\boldsymbol{\Delta b}$) and extra energy is sold back (represented by negative $\boldsymbol{u}$) to the grid.

Further, as shown in Table 3.2-3.10 the battery is estimated to work for $\mathbf{14-20}$ years in different case scenarios. The estimations are based on the average cycle life of the battery and number of battery cycles used by the proposed approach for energy trading. For accurate estimations of the battery cycle life, yearly lifetime and revenue a proper battery capacity fading model is required to be designed. The next chapter proposes a battery capacity fading model to properly estimate the performance of the proposed energy trading strategy.

Chapter 4

Battery Modelling

In the previous chapter, the financial performance parameters like Revenue, Gross Profit, Lifetime, etc. (to evaluate the performance of the algorithm) were derived from the cycle life estimations given by the manufacturer. These estimations, generally used by the research community can give over-optimistic performance results. A proper battery capacity fading model can give useful insight about the battery life, which can further be used to derive more accurate performance parameters. Apart from creating an accurate performance estimation benchmark for energy trading algorithms, these capacity fading models can be used to derive a utility based cost model for the battery system, which can further be merged with the core energy trading algorithm to derive a better performing algorithm. This chapter proposes one such capacity fading model. Later on, the model is used to derive a cost model to utilize it within the DBC framework.

4.1 Battery Capacity Fading Model

Capacity fade or capacity loss is a mechanism by which the battery loses some of its capacity with time. This loss can be reversible as well as irreversible and can occur in both active and inactive battery state. The acceptable irreversible capacity fade depends on the battery application. For energy trading based applications, a net capacity fade less than **30**% is considered to be acceptable. After that, the battery cells are required to be replaced. Due to high energy density, high power density, and larger overall cycle life, rechargeable lithium-ion batteries can be a good option for energy trading application[64]. Capacity fading can occur due to two main reasons[65]. The capacity fading due to

lithium ion and material loss is called true capacity fading. On the other hand, the capacity fading loss due to cell impedance growth is called rate capability loss.

Different capacity fade models use linear[66, 67], quadratic[65] or exponential[68, 69] functions to approximate the fading mechanism. Most researchers have found a logarithmic dependence between cycle life and Depth of Discharge (DOD)[70]. The temperature dependence of the capacity fading is generally modelled using Arrhenius equation[71]. In [69], the authors modelled the capacity fading rate ($\boldsymbol{f_d}$) in terms of the charge processed during a particular interval of time. The model approximates $\boldsymbol{f_d}$ in terms of mean of SOC ($\boldsymbol{S_{av}}$) and standard deviation of SOC ($\boldsymbol{S_{dv}}$) during the time interval '$\boldsymbol{t}$'.

Eq.(4.1) estimates the $\boldsymbol{S_{av}(t)}$ during the time interval '$\boldsymbol{t}$'.

$$S_{av}(t) = \frac{1}{\Delta Ah_t} \int_{Ah_t}^{Ah_{t+1}} S(Ah) dAh \tag{4.1}$$

Eq.(4.2) estimates the $\boldsymbol{S_{dv}(t)}$ during the time interval '$\boldsymbol{t}$'.

$$S_{dv}(t) = (\frac{3}{\Delta Ah_t} \int_{Ah_t}^{Ah_{t+1}} (S(Ah) - S_{av})^2)^{1/2} \tag{4.2}$$

$\boldsymbol{f_d(t)}$ for a time interval '$\boldsymbol{t}$' can be calculated using Eq.(4.3).

$$f_d(t) = (k_1.S_{dv}(t).e^{k_2.S_{av}(t)} + k_3.e^{k_4.S_{dv}(t)}).e^{(\frac{-E_a}{R}(\frac{1}{T_t} - \frac{1}{T_{ref}}))} \tag{4.3}$$

Here $\boldsymbol{k_1}$, $\boldsymbol{k_2}$, $\boldsymbol{k_3}$ and $\boldsymbol{k_4}$ are the parameters of the battery fading model. $\boldsymbol{S(Ah)}$ is the SOC of the battery at charge "$\boldsymbol{Ah}$". $\boldsymbol{f_d(t)}$ represents the amount of charge faded (in $\boldsymbol{Ah}$) per amount of charge processed (in $\boldsymbol{Ah}$). $\boldsymbol{R}$ is the gas constant, $\boldsymbol{E_a}$ is the activation energy, $\boldsymbol{T}$ is the current temperature, and $\boldsymbol{T_{ref}}$ is the reference temperature.

For simulating the battery dynamics, "Thundersky Winston LiFePO4 Battery" (Model No: WB-LYP1000AHC(A)) was considered. For finding the value of parameters ($\boldsymbol{k_1}$, $\boldsymbol{k_2}$, $\boldsymbol{k_3}$ and $\boldsymbol{k_4}$) of the battery capacity fading model, the cycle life vs DOD data was taken from [72]. By fitting the fading model on the data, the hyper-parameter values were calculated: $\boldsymbol{k_1 = 0.0265}$, $\boldsymbol{k_2 = -5.925}$, $\boldsymbol{k_3 = 5.837X10^{-5}}$ and $\boldsymbol{k_4 = -42.315}$. Figure 4.1 clearly shows that the predicted model closely follow the actual battery dynamics over the whole DOD interval.

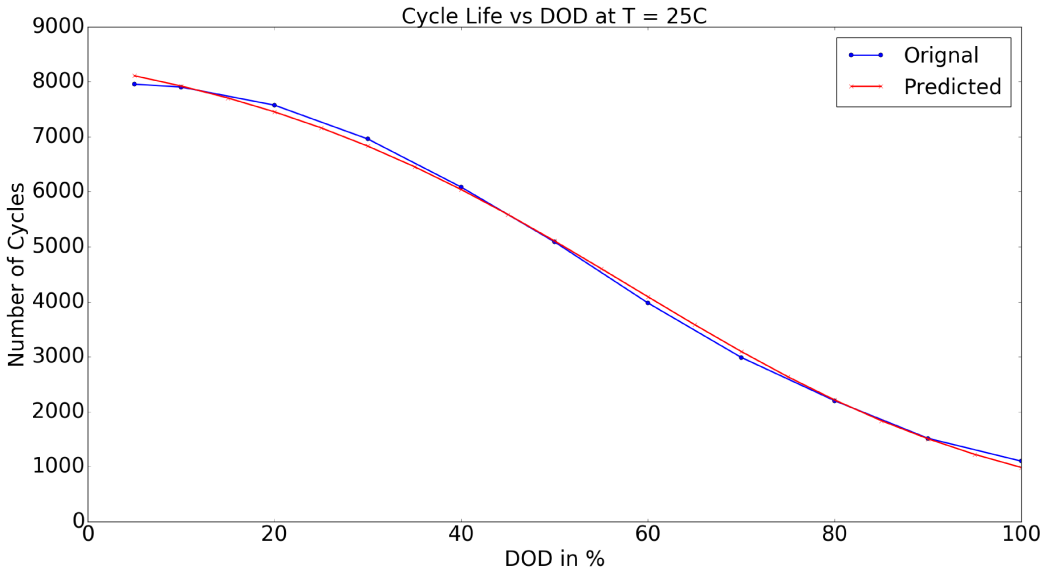

Figure 4.1: Predicted vs Original number of cycles vs DOD curve

4.2 DBC:DE financial performance analysis with Battery Capacity Fading Model

The battery capacity fading model estimated in the previous section can be used to derive more accurate performance parameters, which can be used to better access the expected returns of the investing in the battery for the proposed DBC:DE energy trading strategy.

Performance parameters derived from the fading model are:-

- **$\%f_d$ (in $\%fade/year$)**: This parameter denotes the percentage of battery capacity fade that occurred while using the energy trading strategy over a year. This can be used to derive the other financial parameters and to estimate the battery life more accurately.

- **Profit per 1% fade ($p_2/\%f_d$ in $\$/\%f_d$)**: This is the net profit (p_2: by using the battery system) to capacity fade ($\%f_d$) ratio of the energy trading strategy measured over a year.

- **Revenue (in $)**: This represents the net revenue generated by the battery during its lifetime. It can be calculated by using Eq.(4.4). Unlike the previous chapter (where this parameter was calculated using manufacturer estimated cycle life), here this parameter is calculated using the amount of capacity fade ($\%f_d$) that occurred

during the year. Here ($\mathbf{30}\%$) is the maximum tolerable capacity fade after which the battery is required to be replaced.

$$Revenue = (p_2/\%f_d) * 30\% \tag{4.4}$$

- **Gross Profit (GP in \$)**: This represent the gross profit generated by the battery during its lifetime. It can be calculated by deducting cost of the battery system from the revenue (Eq.(4.5)).

$$GP = Revenue - cost \tag{4.5}$$

- **% Gross Profit (%GP in %)**: This represent the percentage of profit due to investment in battery system. It can be calculated as shown in (Eq.(4.6)).

$$\%GP = 100 * \frac{Revenue - cost}{cost} \tag{4.6}$$

- **Lifetime (in *years*)**: This represents the lifetime of the battery system in years by using a particular strategy. After that, the battery cells are required to be replaced. It can be calculated as shown in (Eq.(4.7)). Here ($\mathbf{30}\%$) is the maximum tolerable capacity fade after which the battery is required to be replaced.

$$Lifetime = 30\%/\%f_d \tag{4.7}$$

Table 4.1 shows the values of the capacity fading model based performance parameters for the DBC:DE strategy (best performing energy trading strategy) in all 9 cases. Clearly, the revenue and battery lifetime estimations highly deviate from the manufacturer defined cycle-life based estimations. Instead of generating a positive gross profit here the estimations are predicting negative values (i.e., a gross monetary loss). Further, now the battery is estimated to work for only $\mathbf{5-7}$ years. This is due to inefficiently charging and discharging of the battery by the DBC:DE algorithm in previous simulations, leading to the high amount of capacity fading (as indicated by high $\%\boldsymbol{f_d}$ values in all 9 cases) in the process. To improve the performance of the proposed DBC:DE algorithm the core algorithm is required to be merged with a battery utility based cost model, which can better indicate if the trade in each time-slot is actually profitable. The next section derives one such cost model based on the proposed battery capacity fading model.

Table 4.1: DBC:DE capacity fading derived performance parameters (Ont: Ontario, Cal: California, NY: New York, R: Residential, C: Commercial, I: Industrial)

		$\%f_d$	p_2 ($/year)	$p_2/\%f_d$ ($/%f˙d)	**Revenue** ($)	**GP** ($)	**%GP** (%)	**Lifetime** (years)
Ont	***R***	5.814	150.00	25.8	773.5	-976.5	-55.80	5.16
	C	5.597	73532.65	13125.0	393750.0	-481250.0	-55.00	5.36
	I	5.597	1103638.05	197312.5	5919375.0	-7205625.0	-54.90	5.36
Cal	***R***	4.573	96.51	21.1	633.5	-1116.5	-63.80	6.56
	C	4.202	46080.71	10966.7	329000.0	-546000.0	-62.40	7.14
	I	4.190	690671.74	164937.5	4948125.0	-8176875.0	-62.30	7.16
NY	***R***	4.471	102.43	22.9	687.8	-1062.3	-60.70	6.71
	C	4.225	49515.55	11754.2	352625.0	-522375.0	-59.70	7.10
	I	4.208	743023.66	176750.0	5302500.0	-7822500.0	-59.60	7.13

4.3 Battery Capacity Fading based Cost Model

Capacity Fading Model discussed in section 1.1 can be used to derive a cost function ($c_{f_d}(t)$) for the battery. The cost of using battery in time slot 't' can be calculated by Eq.(4.8).

$$c_{f_d}(t) = f_d(t) * \Delta Ah_t * cpf \tag{4.8}$$

Here cpf is the cost per fade factor (cpf) of the battery. For a particular battery system cpf can be calculated by using Eq.(4.9).

$$cpf = \frac{B_{cost}}{0.3 * B_{capacity}} \tag{4.9}$$

B_{cost} is the total cost of the battery system and ($0.3 * B_{capacity}$) represent the maximum tolerable capacity fade. Here 30% is taken as the maximum tolerable capacity fade after which the battery is considered to be dead and required to be replaced. This can be combined with the previously proposed energy transfer model to formulate an overall objective function for minimization of the consumer's monetary loss. For the battery system used in the simulation, each battery has a nominal capacity of $3kW$. The price of each battery is around 1050\$. So cpf value is around 1.167\$ per Wh capacity fade.

4.4 Modified DBC with Battery Cost Model

The Eq.(4.10) represent the minimization problem at a particular time-slot "τ". Here the highlighted part (within box) represent change in the original minimization problem due to additional battery cost term. Similar change can be seen in optimal battery charge update (Eq.(4.11)) and overall minimization objective equation (Eq.(4.13)). Overall algorithm remains same as Algorithm 1.

$$f_\tau : \min_{\Delta b(\tau)} \frac{1}{T} \sum_{t=\tau}^{\tau+T-1} [\beta * p_t(\tau) * [\Delta b_t(\tau) + d_t(\tau) - s_t(\tau)] + \boxed{f_d(t) * \Delta Ah_t * cpf}] \quad s.t.((3.16)), ((3.17)), ((3.18)) \tag{4.10}$$

$$\Delta b^*(\tau) = \underset{\Delta b(\tau)}{\operatorname{argmin}} \frac{1}{T} \sum_{t=\tau}^{\tau+T-1} [\beta * p_t(\tau) * [\Delta b_t(\tau) + d_t(\tau) - s_t(\tau)] + \boxed{f_d(t) * \Delta Ah_t * cpf}] \quad s.t.((3.16)), ((3.17)), ((3.18)) \tag{4.11}$$

$$b^*_\tau = b^*_{\tau-1} + \Delta b^*_\tau(\tau) \tag{4.12}$$

$$\begin{aligned} F_\tau(\Delta b) = \frac{1}{T} \sum_{t=\tau}^{\tau+T-1} [\beta * p_t(\tau) * [\Delta b_t(\tau) + d_t(\tau) - s_t(\tau)] + \boxed{f_d(t) * \Delta Ah_t * cpf}] \\ + c_1 * (b(t) - b^{min})^2 + c_2 * (b^{capacity} - b(t))^2 + c_3 * (\Delta b(t) - db^{drate})^2 \\ + c_4 * (db^{crate} - \Delta b(t))^2 + c_5 * (b(t) + \Delta b(t) - b_{min})^2] \end{aligned} \tag{4.13}$$

The simulation results using modified DBC:DE strategy are summarized in Table 4.2 which shows the values of the performance parameters for all 9 cases. Instead of giving a negative gross profit the modification is able to generate $\mathbf{55-70}\%$ profit in all 9 test cases. Although the yearly profit $\boldsymbol{p_2}$ is reduced by $\mathbf{70-75}\%$, the low value of yearly capacity fade ($\%\boldsymbol{f_d}$) ultimately leads to much a higher gross profit. Due to extremely low yearly capacity fading $\mathbf{0.25-0.4}\%$, the life of the battery is increased to $\mathbf{70-120}$ years. But this leads to a very high investment recovery time. In the tested scenarios the investment recovery time is between $\mathbf{50-70}$ years depending on the scenario. This is due to high amount of fading cost penalty used in the new objective function. A more efficient way could be to weigh down the fading cost factor in the objective function. The next chapters simulates such a weighted fading cost model and tries to find the optimal value of the weight.

Table 4.2: Modified DBC:DE performance parameters (Ont: Ontario, Cal: California, NY: New York, R: Residential, C: Commercial, I: Industrial)

		$\%f_d$	p_2 ($/year)	$p_2/\%f_d$ ($/%f d)	**Revenue** ($)	**GP** ($)	**%GP** (%)	**Lifetime** (years)
Ont	***R***	0.414	37.98	91.7	2750.2	1000.2	57.15	72.41
	C	0.406	18709.11	46108.4	1383252.6	508252.6	58.09	73.93
	I	0.405	280527.94	692384.2	20771525.2	7646525.2	58.26	74.04
Cal	***R***	0.264	25.33	96.1	2883.2	1133.2	64.76	113.83
	C	0.258	12702.79	49312.1	1479361.8	604361.8	69.07	116.46
	I	0.251	184714.18	736223.2	22086695.3	8961695.3	68.28	119.57
NY	***R***	0.319	30.39	95.1	2853.6	1103.6	63.06	93.91
	C	0.309	14802.84	47862.5	1435875.0	560875.0	64.10	97.00
	I	0.314	224142.93	714577.0	21437309.0	8312309.0	63.33	95.64

Chapter 5

Weighted Capacity Fading based modified DBC

In the previous chapter, simulations of the capacity fading based modified DBC algorithm resulted in high returns in all test cases. But due to low usage of the battery (as indicated by extremely low yearly capacity fading), the investment recovery rate was extremely high. To solve the problem of effective utilization of the battery resources this chapter simulates a weighted version of the previous strategy. The modification is done in the fading based cost of the objective function, by multiplying the cost with a weight factor called Fading Cost Coefficient w_f. The chapter includes the test to find out the good value of the hyper-parameter w_f.

5.1 Modified DBC with weighted Battery Cost Model

The Eq.(5.1) represent the modified minimization problem at a particular time-slot "τ". Here the highlighted part (within the box) represents change in the original minimization problem due to weighing down the battery cost term. Value of w_f is between 0 and 1. This is to reduce the effect of the fading cost component in the overall objective function. Similar change can be seen in optimal battery charge update (Eq.(5.2)) and overall minimization objective equation (Eq.(5.4)). Overall algorithm remains same as Algorithm 1.

$$f_\tau : \min_{\Delta b(\tau)} \frac{1}{T} \sum_{t=\tau}^{\tau+T-1} [\beta * p_t(\tau) * [\Delta b_t(\tau) + d_t(\tau) - s_t(\tau)] + \boxed{w_f * f_d(t) * \Delta Ah_t * cpf}] \quad s.t.((3.16)), ((3.17)), ((3.18)) \tag{5.1}$$

$$\Delta b^*(\tau) = \underset{\Delta b(\tau)}{\operatorname{argmin}} \frac{1}{T} \sum_{t=\tau}^{\tau+T-1} [\beta * p_t(\tau) * [\Delta b_t(\tau) + d_t(\tau) - s_t(\tau)] + \boxed{w_f * f_d(t) * \Delta Ah_t * cpf}] \quad s.t.((3.16)), ((3.17)), ((3.18)) \tag{5.2}$$

$$b^*_\tau = b^*_{\tau-1} + \Delta b^*_\tau(\tau) \tag{5.3}$$

$$\begin{aligned} F_\tau(\Delta b) = \frac{1}{T} \sum_{t=\tau}^{\tau+T-1} [\beta * p_t(\tau) * [\Delta b_t(\tau) + d_t(\tau) - s_t(\tau)] + \boxed{w_f * f_d(t) * \Delta Ah_t * cpf}] \\ + c_1 * (b(t) - b^{min})^2 + c_2 * (b^{capacity} - b(t))^2 + c_3 * (\Delta b(t) - db^{drate})^2 \\ + c_4 * (db^{crate} - \Delta b(t))^2 + c_5 * (b(t) + \Delta b(t) - b_{min})^2] \end{aligned} \tag{5.4}$$

For finding the optimal value of $\boldsymbol{w_f}$ the Ontario Commercial case was tested with different values of the $\boldsymbol{w_f}$ coefficient. $\boldsymbol{w_f}$ value were varied between $\mathbf{0}$ and $\mathbf{1}$ with a step size of $\mathbf{0.1}$. At $\boldsymbol{w_f} = \mathbf{0}$ the simulation is same as discussed in Chapter 2 and at $\boldsymbol{w_f} = \mathbf{1}$ its same as in Chapter 3. Figure 5.1 shows the effect of $\boldsymbol{w_f}$ coefficient on yearly fading $\%\boldsymbol{f_d}$. Clearly, with increase in $\boldsymbol{w_f}$ the $\%\boldsymbol{f_d}$ value decreases. The reduction in $\%\boldsymbol{f_d}$ is more at lower values of $\boldsymbol{w_f}$ and it gets saturated after $\boldsymbol{w_f} = \mathbf{0.6}$.

Figure 5.2 and 5.3 shows the effect of $\boldsymbol{w_f}$ coefficient on gross profit ($\%\boldsymbol{GP}$) and revenue in the Ontario Commercial Scenario. Clearly, both $\%\boldsymbol{GP}$ and revenue increases with increase in $\boldsymbol{w_f}$. This is due to high amount of reduction in $\%\boldsymbol{f_d}$. Similar effect of high reduction in $\%\boldsymbol{f_d}$ can also be seen on Cumulative Profit per $\%\boldsymbol{f_d}$ ratio. Despite decrease in Cumulative profit ($\boldsymbol{p_2}$) (Figure 5.4), with decrease in $\boldsymbol{w_f}$ the Cumulative Profit per $\%\boldsymbol{f_d}$ ratio gets increased (Figure 5.5).

Figure 5.6 shows the effect of $\boldsymbol{w_f}$ coefficient on the investment recovery time. As shown in in Figure 5.6, the investment recovery is only possible at $\boldsymbol{w_f} > \mathbf{0.2}$. The minimum investment time occurs at $\boldsymbol{w_f} = \mathbf{0.2}$, where the investment is recovered in around $\mathbf{18}$ years. For later simulations the value of $\boldsymbol{w_f}$ is taken as $\mathbf{0.2}$. Table 5.1 summarizes the effect of $\boldsymbol{w_f}$ coefficient on various financial performance parameters as discussed before.

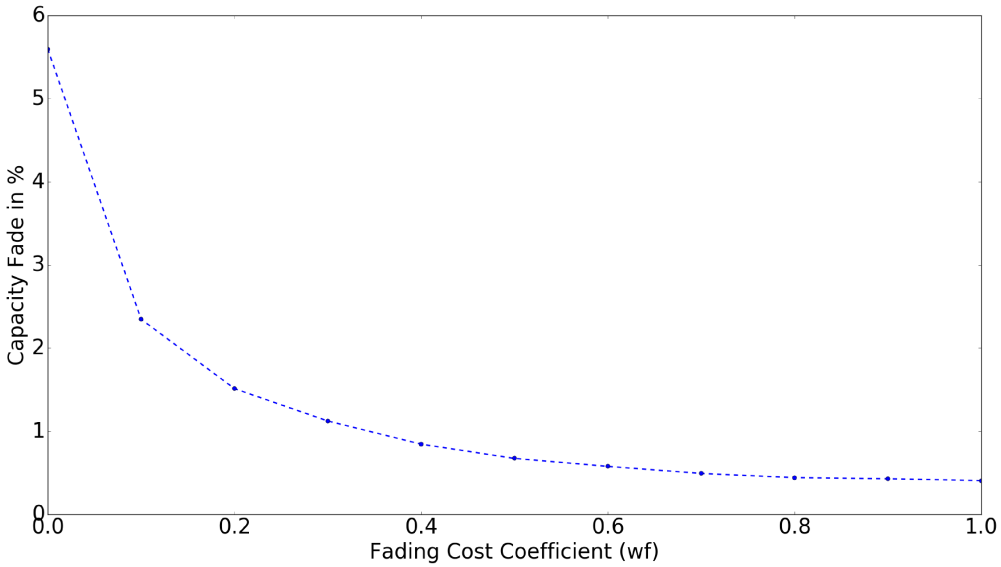

Figure 5.1: Yearly fading $\%\boldsymbol{f_d}$ vs $\boldsymbol{w_f}$

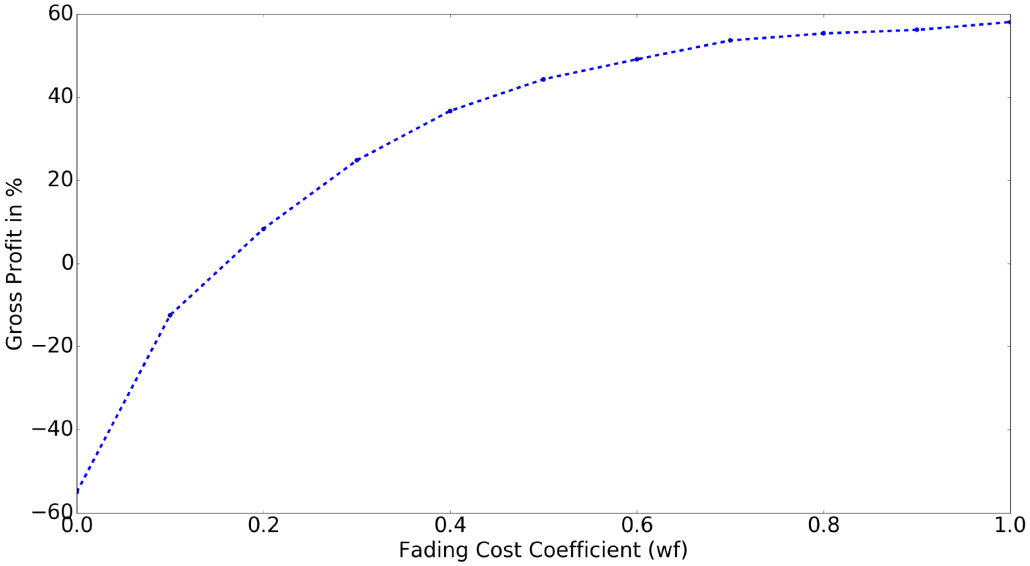

Figure 5.2: % Gross Profit $\%\boldsymbol{GP}$ vs $\boldsymbol{w_f}$

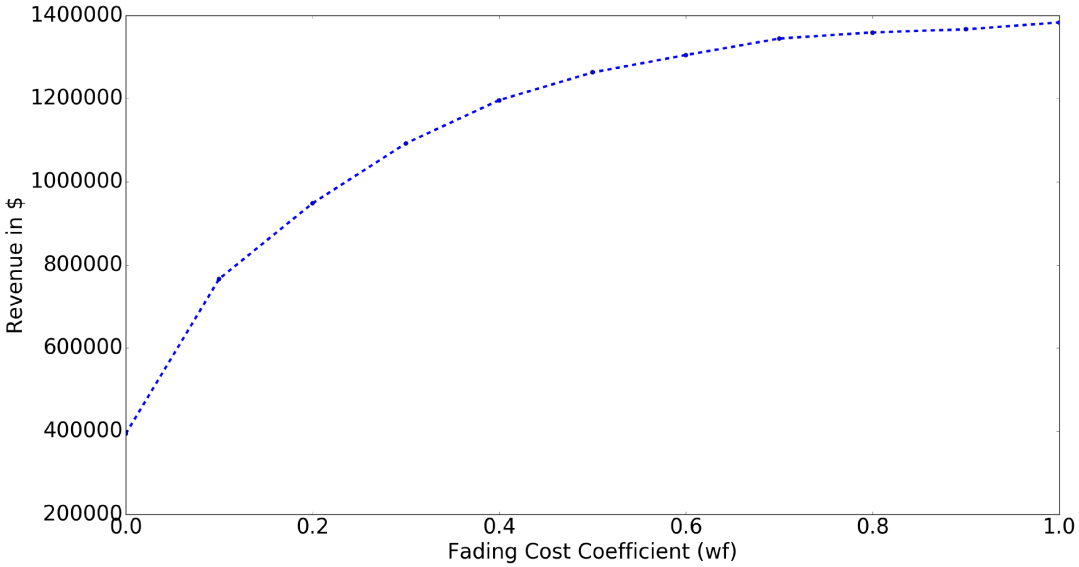

Figure 5.3: Revenue vs w_f

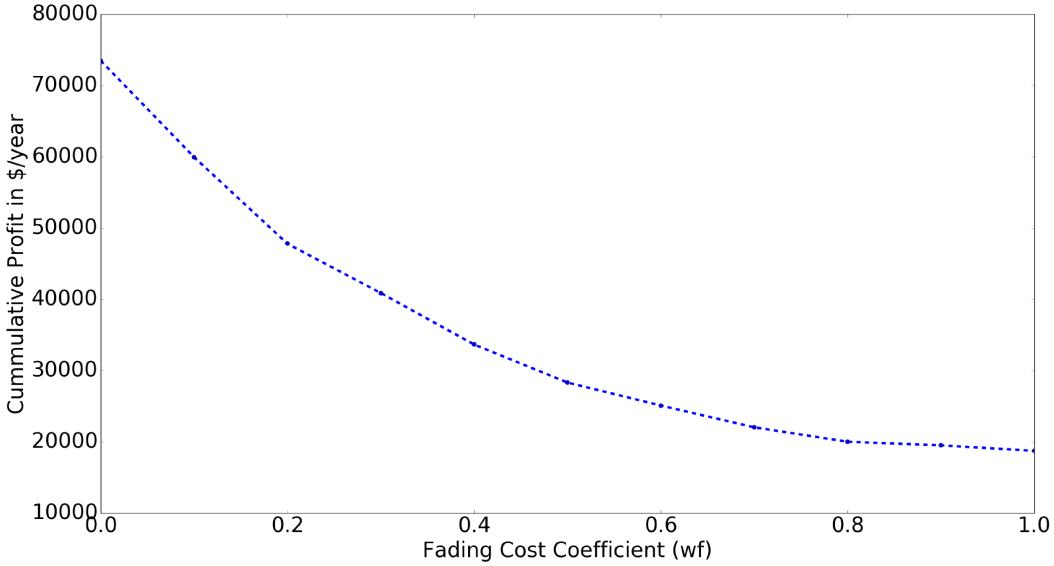

Figure 5.4: Yearly Cumulative Profit p_2 vs w_f

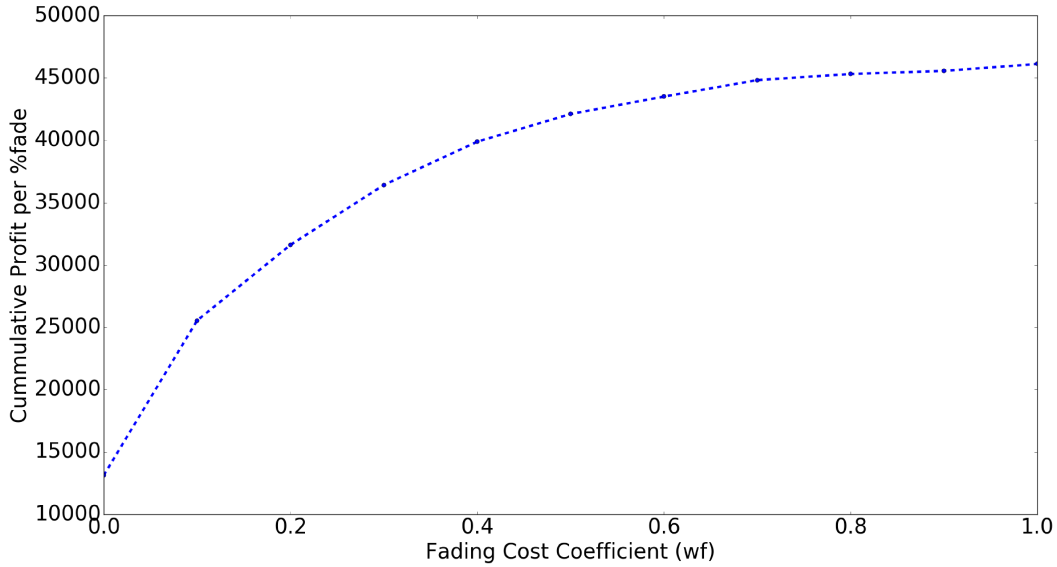

Figure 5.5: Cumulative Profit per %fade vs $\boldsymbol{w_f}$

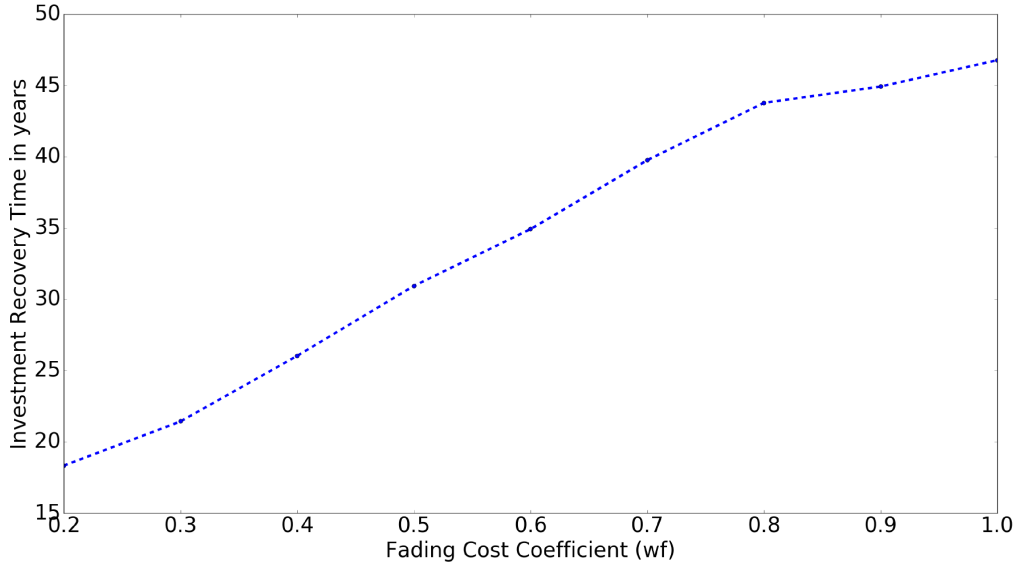

Figure 5.6: Investment Recovery time vs $\boldsymbol{w_f}$

Table 5.1: Effect of change in w_f on DBC performance

w_f	%fd	p2 ($/year)	p2/%fd ($/%fade)	Revenue ($)	GP ($)	%GP (%)	Lifetime (years)	Recovery (years)
0.0	5.60	73460.8	13125.0	393750.0	-481250.0	-55.0	5.4	
0.1	2.35	59920.9	25540.6	766219.5	-108780.5	-12.4	12.8	
0.2	1.51	47769.7	31601.3	948038.6	73038.6	8.3	19.8	18.3
0.3	1.12	40854.6	36404.5	1092136.1	217136.1	24.8	26.7	21.4
0.4	0.84	33628.5	39875.8	1196273.8	321273.8	36.7	35.6	26.0
0.5	0.67	28295.4	42096.9	1262906.9	387906.9	44.3	44.6	30.9
0.6	0.58	25064.0	43494.1	1304823.6	429823.6	49.1	52.1	34.9
0.7	0.49	22014.0	44815.8	1344472.5	469472.5	53.7	61.1	39.7
0.8	0.44	19990.8	45307.9	1359237.3	484237.3	55.3	68.0	43.8
0.9	0.43	19481.5	45554.9	1366645.9	491645.9	56.2	70.2	44.9
1.0	0.41	18709.1	46108.4	1383252.6	508252.6	58.1	73.9	46.8

5.2 Simulation Result

The value of fading cost coefficient 'w_f' was taken as 0.2 as per the simulations done in the previous section. The table 5.2 shows the performance parameter values for all 9 test cases obtained by simulating the weighted DBC:DE strategy. Although the gross profit $\%GP$ has decreased substantially compared to the non-weighted DBC:DE strategy discussed in Chapter 3, it is still positive unlike the vanilla (zero-weighted) DBC:DE strategy discussed in Chapter 2 where it was negative. Further, the value of Cumulative Profit (p_2) is much higher than that in non-weighted DBC:DE strategy, almost comparable to that in vanilla DBC:DE strategy. Table 5.3 shows the improvement in the investment recovery time in comparison to the non-weighted DBC:DE strategy. Using the optimal weight the investment recovery time has reduced by $60 - 70\%$. Now the recovery time is around $18 - 21$ years.

Table 5.2: Weighted fading cost based modified DBC:DE: Performance Parameters (Ont: Ontario, Cal: California, NY: New York, R: Residential, C: Commercial, I: Industrial)

		$\%f_d$	p_2 ($/year)	$p_2/\%f_d$ ($/%f d)	**Revenue** ($)	**GP** ($)	**%GP** (%)	**Lifetime** (years)
Ont	***R***	1.542	95.83	62.1	1864.2	114.2	6.53	19.45
	C	1.512	47769.73	31601.3	948038.6	73038.6	8.35	19.85
	I	1.481	695840.94	469906.9	14097208.5	972208.5	7.41	20.26
Cal	***R***	1.336	86.33	64.6	1938.8	188.8	10.79	22.46
	C	1.262	41075.29	32558.0	976739.1	101739.1	11.63	23.78
	I	1.279	611133.66	477872.9	14336186.2	1211186.2	9.23	23.46
NY	***R***	1.360	86.98	64.0	1918.9	168.9	9.65	22.06
	C	1.317	42569.47	32330.8	969923.7	94923.7	10.85	22.78
	I	1.352	645515.79	477420.1	14322603.7	1197603.7	9.12	22.19

Table 5.3: Investment Recovery Time (in years)

		w_f **= 1.0 (non-weighted)**	w_f **= 0.2**	**%change**
Ontario	***Residential***	46.07	18.26	60.36
	Commercial	46.77	18.32	60.83
	Industrial	46.79	18.86	59.69
California	***Residential***	69.09	20.27	70.66
	Commercial	68.88	21.30	69.07
	Industrial	71.06	21.48	69.78
New-York	***Residential***	57.59	20.12	65.06
	Commercial	59.11	20.55	65.23
	Industrial	58.56	20.33	65.28

Chapter 6

Conclusion and Future Work

The study proposed a Dynamic Programming based framework called Dynamic Battery Charging (DBC) Algorithm for Energy Trading from the end-user perspective. The end-user was assumed to possess a PV system for electricity generation, a battery system for electricity storage and a load. Further, the grid was allowed to have a bi-directional electricity trade with the end-user. An energy balancing model called energy transfer model was developed to incorporate within the DBC framework. The framework utilizes an optimization algorithm to find out the optimal battery charge state dynamically. The basic framework was tested using two optimization algorithms: Differential Evolution (DBC:DE) and Momentum based Gradient Descent (DBC:GD). The test bed included three different load profiles (Residential, Commercial, and Industrial) and three different electricity markets (Ontario, California, and New York, thus accounting for nine different test cases. The hourly price, solar and load data in these cases was used to train machine learning tools called support vector machine (SVM). The hourly traces of electricity price, harvested energy and electricity demand derived from the trained SVM was used with the DBC framework to find the optimal battery charge states. The performance of the DBC:DE and DBC:GD based approach was tested against the Reinforcement Learning based energy trading approach and two other end-user scenarios.

In all the nine cases the DBC:DE algorithm outperformed other approaches. To further improve the proposed framework, a battery capacity fading based battery cost model was developed and incorporated into the basic framework. This was done to get better estimations of the profitability of each trade utilizing the battery. The performance of the framework was evaluated using various monetary and battery lifetime based performance

parameters. Further improvements were done by weighing down the battery cost model using the fading cost Coefficient (w_f).

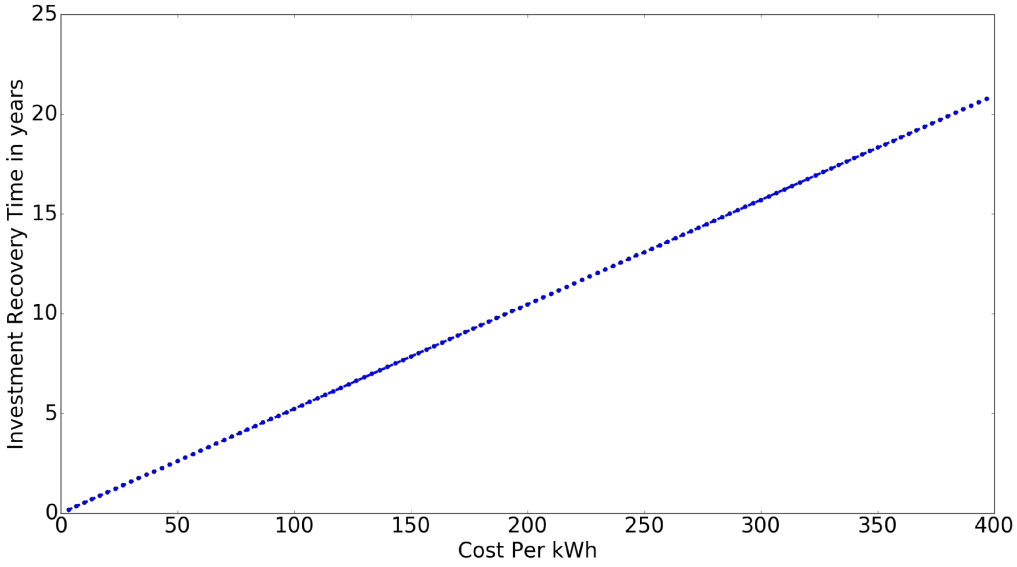

Figure 6.1: Investment Recovery Time vs Battery Cost per kWh

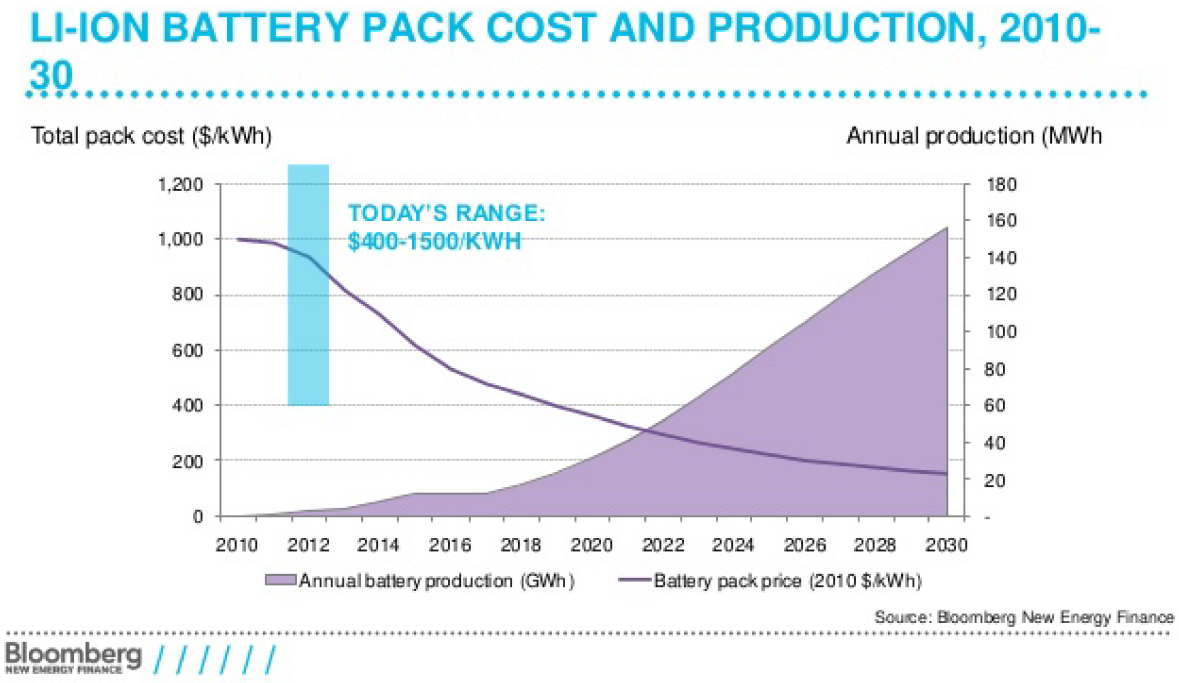

Figure 6.2: Battery Cost per kWh forecast

Although the proposed strategy works well in recovering the battery investment money, **18** years is still more than what can actually be considered a profitable investment. This is mainly due to the high battery cost per kWh in the present scenario. The

tested battery would cost around $\mathbf{350\$/kWh}$. Figure 6.1 shows the estimated investment recovery time at different battery cost per kWh ratio. The relationship between the two factors is linear and the investment recovery time is directly proportional to the cost per kWh ratio. To lower down the investment recovery time to 10 years the battery cost had to reduce to $\mathbf{200\$/kWh}$.

Last few years have witnessed a significant reduction in the battery cost. The battery cost per kWh has decreased by more than **50**% in last **8** years and according to the Bloomberg New Energy Finance Report (Figure 6.2) it is going to get below $\mathbf{200\$/kWh}$ by the year **2023**. That's a good sign for the investment in the battery systems for energy trading in future. So, by the year **2023**, the battery investment recovery time using the proposed strategy would reduce below **10** years. The cost is further estimated to go below $\mathbf{100\$/kWh}$ around the year **2030**. This would further reduce the battery investment recovery time to **5** years. This proves the utility of the proposed strategy in the future energy markets.

6.1 Summary of Contributions

The proposed framework models the monetary loss of trading electricity in a certain timeslot. Using the loss model and forecasted values of the electricity price, load demand and solar harvest, the framework predicts the optimal sequence of decision in the form of charging/discharging of the battery system (or amount of electricity to be traded) by minimizing the monetary loss over that sequence.

6.2 Future Work

The current energy trading framework, designed for a PV system, can be modified to work for an Electric Vehicle. But that would require re-tuning of the various hyper-parameters like fading cost coefficient (w_f) as the battery system used in these system has a lower depth of discharge (unlike the deep cycle batteries used in PV systems) and are of much lower cost (already below $100\$/kWh$). The framework was designed to work using non-gradient and gradient techniques. Further modification can enable usage of advanced learning techniques like Trust Region Policy Optimization (TRPO) [73], which unlike

Q-learning, can generate continuous actions (control outputs in this case). Further, work can be done to build advanced estimators like neural networks by using meteorological geographical features (like weather conditions) along with the temporal features used in this study.

References

[1] C. Frei, R. Whitney, H.-W. Schiffer, K. Rose, D. A. Rieser, A. Al-Qahtani, P. Thomas, H. Turton, M. Densing, E. Panos, *et al.*, "World energy scenarios: Composing energy futures to 2050," tech. rep., Conseil Francais de l'energie, 2013.

[2] U. Lehr, C. Lutz, and D. Edler, "Green jobs? economic impacts of renewable energy in germany," *Energy Policy*, vol. 47, pp. 358–364, 2012.

[3] M. Bhattacharya, S. R. Paramati, I. Ozturk, and S. Bhattacharya, "The effect of renewable energy consumption on economic growth: Evidence from top 38 countries," *Applied Energy*, vol. 162, pp. 733–741, 2016.

[4] B. V. Mathiesen, H. Lund, and K. Karlsson, "100% renewable energy systems, climate mitigation and economic growth," *Applied Energy*, vol. 88, no. 2, pp. 488–501, 2011.

[5] T. Adefarati and R. Bansal, "Integration of renewable distributed generators into the distribution system: a review," *IET Renewable Power Generation*, vol. 10, no. 7, pp. 873–884, 2016.

[6] L. E. Jones, *Renewable energy integration: practical management of variability, uncertainty, and flexibility in power grids.* Academic Press, 2017.

[7] P. Denholm and M. Hand, "Grid flexibility and storage required to achieve very high penetration of variable renewable electricity," *Energy Policy*, vol. 39, no. 3, pp. 1817–1830, 2011.

[8] Y. Wang, V. Silva, and M. Lopez-Botet-Zulueta, "Impact of high penetration of variable renewable generation on frequency dynamics in the continental europe in-

terconnected system," *IET Renewable Power Generation*, vol. 10, no. 1, pp. 10–16, 2016.

[9] P. Denholm and R. M. Margolis, "Evaluating the limits of solar photovoltaics (pv) in traditional electric power systems," *Energy policy*, vol. 35, no. 5, pp. 2852–2861, 2007.

[10] A. Solomon, D. M. Kammen, and D. Callaway, "Investigating the impact of wind–solar complementarities on energy storage requirement and the corresponding supply reliability criteria," *Applied Energy*, vol. 168, pp. 130–145, 2016.

[11] V. C. Gungor, D. Sahin, T. Kocak, S. Ergut, C. Buccella, C. Cecati, and G. P. Hancke, "A survey on smart grid potential applications and communication requirements," *IEEE Transactions on Industrial Informatics*, vol. 9, no. 1, pp. 28–42, 2013.

[12] D. E. Olivares, A. Mehrizi-Sani, A. H. Etemadi, C. A. Cañizares, R. Iravani, M. Kazerani, A. H. Hajimiragha, O. Gomis-Bellmunt, M. Saeedifard, R. Palma-Behnke, *et al.*, "Trends in microgrid control," *IEEE Transactions on smart grid*, vol. 5, no. 4, pp. 1905–1919, 2014.

[13] M. L. Tuballa and M. L. Abundo, "A review of the development of smart grid technologies," *Renewable and Sustainable Energy Reviews*, vol. 59, pp. 710–725, 2016.

[14] H. Farhangi, "The path of the smart grid," *IEEE power and energy magazine*, vol. 8, no. 1, 2010.

[15] P. Palensky and D. Dietrich, "Demand side management: Demand response, intelligent energy systems, and smart loads," *IEEE transactions on industrial informatics*, vol. 7, no. 3, pp. 381–388, 2011.

[16] G. Strbac, "Demand side management: Benefits and challenges," *Energy policy*, vol. 36, no. 12, pp. 4419–4426, 2008.

[17] B. Dunn, H. Kamath, and J.-M. Tarascon, "Electrical energy storage for the grid: a battery of choices," *Science*, vol. 334, no. 6058, pp. 928–935, 2011.

[18] S. J. Kazempour, M. P. Moghaddam, M. Haghifam, and G. Yousefi, "Electric energy storage systems in a market-based economy: Comparison of emerging and traditional technologies," *Renewable energy*, vol. 34, no. 12, pp. 2630–2639, 2009.

[19] D. Lindley, "Smart grids: The energy storage problem," *Nature News*, vol. 463, no. 7277, pp. 18–20, 2010.

[20] J. Lassila, J. Haakana, V. Tikka, and J. Partanen, "Methodology to analyze the economic effects of electric cars as energy storages," *IEEE Transactions on smart grid*, vol. 3, no. 1, pp. 506–516, 2012.

[21] N. Rotering and M. Ilic, "Optimal plug-in electric vehicle charge control in deregulated electricity markets," *IEEE Transactions on Power Systems*, vol. 26, no. 3, pp. 1021–1029, 2011.

[22] B. Nykvist and M. Nilsson, "Rapidly falling costs of battery packs for electric vehicles," *Nature Climate Change*, vol. 5, no. 4, pp. 329–332, 2015.

[23] A. A. Asif and R. Singh, "Further cost reduction of battery manufacturing," *Batteries*, vol. 3, no. 2, p. 17, 2017.

[24] I. S. Bayram, M. Z. Shakir, M. Abdallah, and K. Qaraqe, "A survey on energy trading in smart grid," in *Signal and Information Processing (GlobalSIP), 2014 IEEE Global Conference on*, pp. 258–262, IEEE, 2014.

[25] E. Sortomme and M. A. El-Sharkawi, "Optimal combined bidding of vehicle-to-grid ancillary services," *IEEE Transactions on Smart Grid*, vol. 3, no. 1, pp. 70–79, 2012.

[26] D. Ilic, P. G. Da Silva, S. Karnouskos, and M. Griesemer, "An energy market for trading electricity in smart grid neighbourhoods," in *Digital Ecosystems Technologies (DEST), 2012 6th IEEE International Conference on*, pp. 1–6, IEEE, 2012.

[27] P. Vytelingum, S. D. Ramchurn, T. D. Voice, A. Rogers, and N. R. Jennings, "Trading agents for the smart electricity grid," in *Proceedings of the 9th International Conference on Autonomous Agents and Multiagent Systems: volume 1-Volume 1*, pp. 897–904, International Foundation for Autonomous Agents and Multiagent Systems, 2010.

[28] Y. Wang, W. Saad, Z. Han, H. V. Poor, and T. Başar, "A game-theoretic approach to energy trading in the smart grid," *IEEE Transactions on Smart Grid*, vol. 5, no. 3, pp. 1439–1450, 2014.

[29] A. Y. Lam, L. Huang, A. Silva, and W. Saad, "A multi-layer market for vehicle-to-grid energy trading in the smart grid," in *Computer Communications Workshops (INFOCOM WKSHPS), 2012 IEEE Conference on*, pp. 85–90, IEEE, 2012.

[30] I. S. Bayram, G. Michailidis, I. Papapanagiotou, and M. Devetsikiotis, "Decentralized control of electric vehicles in a network of fast charging stations," in *Global Communications Conference (GLOBECOM), 2013 IEEE*, pp. 2785–2790, IEEE, 2013.

[31] W. Tushar, J. A. Zhang, D. B. Smith, H. V. Poor, and S. Thiébaux, "Prioritizing consumers in smart grid: A game theoretic approach," *IEEE Transactions on Smart Grid*, vol. 5, no. 3, pp. 1429–1438, 2014.

[32] W. Tushar, W. Saad, H. V. Poor, and D. B. Smith, "Economics of electric vehicle charging: A game theoretic approach," *IEEE Transactions on Smart Grid*, vol. 3, no. 4, pp. 1767–1778, 2012.

[33] W. Saad, Z. Han, H. V. Poor, and T. Başar, "A noncooperative game for double auction-based energy trading between phevs and distribution grids," in *Smart Grid Communications (SmartGridComm), 2011 IEEE International Conference on*, pp. 267–272, IEEE, 2011.

[34] B.-G. Kim, S. Ren, M. van der Schaar, and J.-W. Lee, "Bidirectional energy trading and residential load scheduling with electric vehicles in the smart grid," *IEEE Journal on Selected Areas in Communications*, vol. 31, no. 7, pp. 1219–1234, 2013.

[35] C. Wu, H. Mohsenian-Rad, and J. Huang, "Vehicle-to-aggregator interaction game," *IEEE Transactions on Smart Grid*, vol. 3, no. 1, pp. 434–442, 2012.

[36] Y. Wang, W. Saad, Z. Han, H. V. Poor, and T. Başar, "A game-theoretic approach to energy trading in the smart grid," *IEEE Transactions on Smart Grid*, vol. 5, no. 3, pp. 1439–1450, 2014.

[37] S. Chen, N. B. Shroff, and P. Sinha, "Energy trading in the smart grid: From end-user's perspective," in *Signals, Systems and Computers, 2013 Asilomar Conference on*, pp. 327–331, IEEE, 2013.

[38] J. Matamoros, D. Gregoratti, and M. Dohler, "Microgrids energy trading in islanding mode," in *Smart Grid Communications (SmartGridComm), 2012 IEEE Third International Conference on*, pp. 49–54, IEEE, 2012.

[39] B. Ramachandran, S. K. Srivastava, C. S. Edrington, and D. A. Cartes, "An intelligent auction scheme for smart grid market using a hybrid immune algorithm," *IEEE Transactions on Industrial Electronics*, vol. 58, no. 10, pp. 4603–4612, 2011.

[40] H. Akhavan-Hejazi and H. Mohsenian-Rad, "A stochastic programming framework for optimal storage bidding in energy and reserve markets," in *Innovative Smart Grid Technologies (ISGT), 2013 IEEE PES*, pp. 1–6, IEEE, 2013.

[41] P. P. Reddy and M. M. Veloso, "Strategy learning for autonomous agents in smart grid markets," in *IJCAI Proceedings-International Joint Conference on Artificial Intelligence*, vol. 22, p. 1446, 2011.

[42] M. Peters, W. Ketter, M. Saar-Tsechansky, and J. Collins, "Autonomous data-driven decision-making in smart electricity markets," in *Joint European Conference on Machine Learning and Knowledge Discovery in Databases*, pp. 132–147, Springer, 2012.

[43] H. Wang, T. Huang, X. Liao, H. Abu-Rub, and G. Chen, "Reinforcement learning for constrained energy trading games with incomplete information," *IEEE Transactions on Cybernetics*, 2016.

[44] A. S. Poznyak and K. Najim, *Learning automata and stochastic optimization.* 1997.

[45] D. Urieli and P. Stone, "Tactex'13: a champion adaptive power trading agent," in *Proceedings of the 2014 international conference on Autonomous agents and multi-agent systems*, pp. 1447–1448, International Foundation for Autonomous Agents and Multiagent Systems, 2014.

[46] H. Wang, T. Huang, X. Liao, H. Abu-Rub, and G. Chen, "Reinforcement learning in energy trading game among smart microgrids," *IEEE Transactions on Industrial Electronics*, vol. 63, no. 8, pp. 5109–5119, 2016.

[47] P. P. Reddy and M. M. Veloso, "Learned behaviors of multiple autonomous agents in smart grid markets.," in *AAAI*, 2011.

[48] "Independent electricity system operator," *http://www.ieso.ca*.

[49] "California iso," *http://oasis.caiso.com*.

[50] "New york independent system operator," *http://www.nyiso.com*.

[51] N. I. Sapankevych and R. Sankar, "Time series prediction using support vector machines: a survey," *IEEE Computational Intelligence Magazine*, vol. 4, no. 2, 2009.

[52] J. Che and J. Wang, "Short-term electricity prices forecasting based on support vector regression and auto-regressive integrated moving average modeling," *Energy Conversion and Management*, vol. 51, no. 10, pp. 1911–1917, 2010.

[53] E. Ceperic, V. Ceperic, and A. Baric, "A strategy for short-term load forecasting by support vector regression machines," *IEEE Transactions on Power Systems*, vol. 28, no. 4, pp. 4356–4364, 2013.

[54] J. Zeng and W. Qiao, "Short-term solar power prediction using a support vector machine," *Renewable Energy*, vol. 52, pp. 118–127, 2013.

[55] G. Goh, "Why momentum really works," *Distill*, vol. 2, no. 4, p. e6, 2017.

[56] K. Fleetwood, "An introduction to differential evolution," in *Proceedings of Mathematics and Statistics of Complex Systems (MASCOS) One Day Symposium, 26th November, Brisbane, Australia*, 2004.

[57] L. P. Kaelbling, M. L. Littman, and A. W. Moore, "Reinforcement learning: A survey," *Journal of artificial intelligence research*, vol. 4, pp. 237–285, 1996.

[58] V. Mnih, K. Kavukcuoglu, D. Silver, A. Graves, I. Antonoglou, D. Wierstra, and M. Riedmiller, "Playing atari with deep reinforcement learning," *arXiv preprint arXiv:1312.5602*, 2013.

[59] "National solar radiation database," *https://nsrdb.nrel.gov/*.

[60] "National renewable energy laboratory," *http://www.nrel.gov*.

[61] M. Sengupta, A. Habte, P. Gotseff, A. Weekley, A. Lopez, M. Anderberg, C. Molling, and A. Heidinger, "Physics-based goes product for use in nrel's national solar radiation database: Preprint," tech. rep., NREL (National Renewable Energy Laboratory (NREL), Golden, CO (United States)), 2014.

[62] A. Habte, M. Sengupta, and A. Lopez, "Evaluation of the national solar radiation database (nsrdb): 1998–2015," tech. rep., NREL (National Renewable Energy Laboratory (NREL), Golden, CO (United States)), 2017.

[63] C. B. E. Efficiency, "Walmart—saving energy, saving money through comprehensive retrofits.,"

[64] L. Lu, X. Han, J. Li, J. Hua, and M. Ouyang, "A review on the key issues for lithium-ion battery management in electric vehicles," *Journal of power sources*, vol. 226, pp. 272–288, 2013.

[65] P. Ramadass, B. Haran, R. White, and B. N. Popov, "Mathematical modeling of the capacity fade of li-ion cells," *Journal of Power Sources*, vol. 123, no. 2, pp. 230–240, 2003.

[66] Y. Zhang and C.-Y. Wang, "Cycle-life characterization of automotive lithium-ion batteries with linio2 cathode," *Journal of the Electrochemical Society*, vol. 156, no. 7, pp. A527–A535, 2009.

[67] F. P. Tredeau and Z. M. Salameh, "Evaluation of lithium iron phosphate batteries for electric vehicles application," in *Vehicle Power and Propulsion Conference, 2009. VPPC'09. IEEE*, pp. 1266–1270, IEEE, 2009.

[68] A. Millner, "Modeling lithium ion battery degradation in electric vehicles," in *Innovative Technologies for an Efficient and Reliable Electricity Supply (CITRES), 2010 IEEE Conference on*, pp. 349–356, IEEE, 2010.

[69] L. Lam and P. Bauer, "Practical capacity fading model for li-ion battery cells in electric vehicles," *IEEE transactions on power electronics*, vol. 28, no. 12, pp. 5910–5918, 2013.

[70] G. Ning and B. N. Popov, "Cycle life modeling of lithium-ion batteries," *Journal of The Electrochemical Society*, vol. 151, no. 10, pp. A1584–A1591, 2004.

[71] R. Spotnitz, "Simulation of capacity fade in lithium-ion batteries," *Journal of Power Sources*, vol. 113, no. 1, pp. 72–80, 2003.

[72] "Lithium solar power lifepo4." `http://gwl-power.tumblr.com/post/140925159571/the-cycle-life-of-winston-batttery-cells-versus`.

[73] J. Schulman, S. Levine, P. Abbeel, M. Jordan, and P. Moritz, "Trust region policy optimization," in *International Conference on Machine Learning*, pp. 1889–1897, 2015.